

## Article

# Comparison of Performance Analysis Results with Developed Site-Specific Response Spectra and Turkish Seismic Design Code: A Case Study from the SW Türkiye Region

Mehmet Alpyürür \* and Hakan Ulutaş 

Faculty of Engineering and Architecture, Department of Civil Engineering, Burdur Mehmet Akif Ersoy University, Burdur 15030, Türkiye

\* Correspondence: malpyurur@mehmetakif.edu.tr

**Abstract:** On 6 February 2023, the Kahramanmaraş earthquakes clearly showed that the elastic spectrum curves in TBEC-2018 are insufficient to represent earthquake behavior. In this study, the effect of using a site-specific spectrum curve instead of the elastic spectrum given in TBEC-2018 on the earthquake safety of a building is investigated. For this purpose, the provinces in southwest Anatolia, Türkiye, which is one of the most tectonically complex regions with frequent seismic events, were selected. In the first stage of the study, spectrum curves were obtained for earthquakes with return periods of 2475, 475, and 72 years for each of the provinces in this region. These spectrum curves were obtained using probabilistic seismic hazard studies that take into account the active faults of the provinces and earthquake activity in both historical and instrumental periods. In the second stage of the study, analytical models of a selected model RC building were created according to each province, and static pushover analyses of these building models were performed both according to the elastic spectrum given in TBEC-2018 and according to the spectrum curve created specifically for the province. The results of the analyses show that the change in the spectrum changes the target displacement level of the buildings, and as a result, the cross-sectional damage zone of the structural elements under the earthquake effect is changed. So much so that using the site-specific instead of the elastic spectrum given in TBEC-2018 changed the damage zone of 43% of the beams and 26.4% of the columns in the İzmir model. The change in the section damage zones changed the performance level of some floors of the models and the performance level of the building. The study revealed the importance of using the most realistic elastic spectrum curves in order to determine the earthquake performance of buildings that is as close as possible to their behavior in a possible earthquake.

**Keywords:** earthquake; seismic hazard analysis; site-specific spectrum; pushover analysis; SW Türkiye



**Citation:** Alpyürür, M.; Ulutaş, H. Comparison of Performance Analysis Results with Developed Site-Specific Response Spectra and Turkish Seismic Design Code: A Case Study from the SW Türkiye Region. *Buildings* **2024**, *14*, 1233. <https://doi.org/10.3390/buildings14051233>

Academic Editors: Chiara Bedon, Marco Fasan and Nicola Chieffo

Received: 29 February 2024

Revised: 4 April 2024

Accepted: 23 April 2024

Published: 26 April 2024



**Copyright:** © 2024 by the authors. Licensee MDPI, Basel, Switzerland. This article is an open access article distributed under the terms and conditions of the Creative Commons Attribution (CC BY) license (<https://creativecommons.org/licenses/by/4.0/>).

## 1. Introduction

Türkiye is considered to be a nation characterized by a significant level of seismic activity. Türkiye, situated inside the Alp–Himalayan orogenic belt, encounters recurrent and devastating seismic events that lead to significant human casualties and property damage. Past occurrences of earthquakes in Türkiye serve as indicators of the potential occurrence of future seismic events. Regrettably, the magnitude, location, and temporal occurrence of these earthquakes cannot be accurately forecasted, rendering prevention efforts ineffective. In the given scenario, the most rational approach to mitigate potential loss of life and property damage caused by earthquakes is to implement the construction of earthquake-resistant buildings.

The recent seismic events that occurred in Kahramanmaraş, specifically the earthquakes with magnitudes of 7.7 and 7.6, have demonstrated the heightened importance of assessing the potential for seismic activity in populated areas and implementing measures to develop buildings that can withstand earthquakes. These events have resulted in significant human casualties and property damage, underscoring the urgent need for

proactive measures to mitigate seismic risk. The occurrence of severe earthquakes in many regions of the globe presents a significant danger to human civilization. Consequently, it is imperative to consider the hazards associated with earthquakes while constructing buildings and infrastructure [1–4].

The necessity of updating and enhancing seismic hazard maps is paramount in regions characterized by high-risk seismic activity. The initiation of damage mitigation endeavors in Türkiye can be traced back to the seismic event that occurred in Erzincan in 1939. The initial authoritative delineation of seismic regions in Türkiye was established in 1945, and further revisions have been conducted on six occasions thereafter [5–8]. Turkish authorities updated their 1996 Earthquake Zones Map in 2018, and the updated version became official on 1 January 2019. Compared to its predecessors, the latest map was made with more precise information by utilizing the most recent earthquake catalogs, mathematical models, and source parameters. The utilization of the TBEC-2018 [9] code involves the incorporation of this map for the purpose of developing a design spectrum that accounts for various levels of seismic ground motion and site classifications [10–13].

The design spectra of earthquake codes, which are extensively employed in earthquake-resistant building design, are simple to implement but may not always match the actual behavior of an earthquake. These spectra were generated by enveloping the response spectra related to a set of seismic scenarios [14]. In several earthquake scenarios, the horizontal response spectra of earthquakes may exceed the design spectrum. The earthquakes that occurred on 6 February 2023 in Pazarcık ( $M_w = 7.7$ ) and Elbistan ( $M_w = 7.6$ ) resulted in horizontal response spectra that surpassed the TBEC-2018 design spectrum at numerous locations. According to the measurements obtained from Station 3126 and Station 4614 in Antakya (Hatay) and Pazarcık (Kahramanmaraş), the geometric mean of the two horizontal response spectra surpasses the TBEC-2018 design spectrum for a return period of 475 years across most periods. This was particularly the case in areas with high levels of destruction. According to the data presented in Figure 1, the geometric averages of both stations surpass the design spectrum for a return period of 2475 years when considering short periods of less than 0.5 s. These cases show how important it is to perform seismic hazard studies that use site-representative ground motion prediction equations (GMPEs), model the seismic sources in more detail, and calculate the seismicity parameters of these sources precisely.

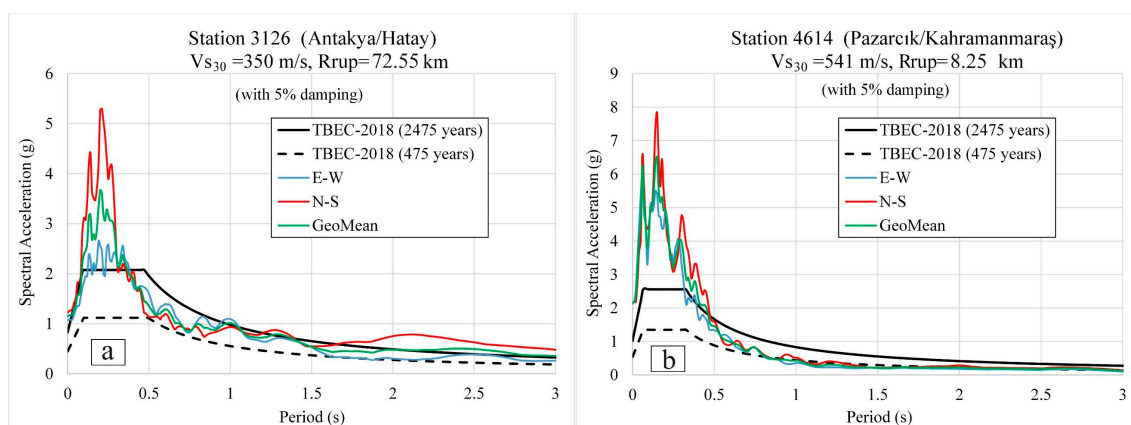


**Figure 1.** Response spectra compared with TBEC-2018 at stations (a) 3126 and (b) 4614, in relation to the Pazarcık earthquake ( $M_w = 7.7$ ).

Seismic risk analysis plays a pivotal role in contemporary pre-earthquake catastrophe management, serving as a vital instrument for informed decision-making. For this purpose, many scholars have undertaken seismic hazard investigations for various geographical areas [15–20]. One of these regions is the SW Türkiye region. Due to its increasing population and growing significance as a cultural, agricultural, commercial, and tourism center, the southwest Türkiye region, which has a high earthquake risk, has received more attention

for its seismic hazard assessments. Various academics have conducted studies to explore the seismic hazard analyses of some provinces in southwest Türkiye, owing to the significant seismic activity seen in the region [21–25]. Spectrum curves developed from previous seismic hazard analyses carried out in the region were developed by taking into account only the bedrock ground and the earthquake level that has a 10% probability of exceedance in 50 years. In this study, a comprehensive seismic hazard analysis was carried out, taking into account local site effects. Spectrum curves were created for the provinces in the region, taking into account different earthquake levels and local site effects.

The performance-based assessment method was first included in earthquake codes in Türkiye with the Turkish Seismic Design Code (TEC-2007) [26], and this method has also found its place in TBEC-2018. One of the most important stages of the performance-based assessment method is the determination of the cross-sections' damage levels of the structural elements. The damage level of the cross-sections is obtained by comparing the deformation value of the cross-sections of the structural elements in the building analyzed by the nonlinear evaluation method with the upper limit values of the deformation corresponding to the cross-sections' damage levels in the regulation [27]. The performance level of the building is determined according to the damage occurring in the cross-sections. There are many studies in the literature on performance-based design [28–31].

The earthquake performance of buildings provides information on whether the building is safe to use in terms of life safety. Buildings that do not provide the target performance level should be strengthened or demolished. Therefore, it is very important to use the most realistic elastic spectrum curves in these analyses in order to obtain earthquake performance results of buildings that are as close as possible to the behavior of the buildings in a possible earthquake. However, the 6 February 2023 Kahramanmaraş earthquakes clearly showed that the elastic spectrum curves in TBEC-2018 are insufficient to represent the earthquake behavior [32–35]. This study presents site-specific spectrum curves that can be used in earthquake performance analyses in the provinces located in the southwestern Anatolia region of Türkiye.

Within the existing body of literature, there have been investigations conducted about the generation of spectrum curves. These studies have explored an alternative approach by taking into account the seismic activity specific to each place, as opposed to relying solely on regional earthquake spectrum curves [36,37]. However, there is no study for SW Türkiye that examines the effect of using a site-specific spectrum curve instead of the elastic spectrum in TBEC-2018 in building performance analysis on building earthquake safety. This study is comprehensive in terms of evaluating the results of seismic hazard analyses and building performance analyses for seven provinces with different tectonic characteristics in SW Türkiye, examining the changes in earthquake and structural parameters, and contributing to studies to be conducted for other regions of Türkiye.

## 2. Geology, Tectonics, and Seismicity of SW Türkiye

Türkiye is on the border of the Arabian and Eurasian tectonic plates. The collision of these plates has resulted in the formation of significant tectonic structures (Figure 2), including the North Anatolian Shear Zone (NASZ), the East Anatolian Shear Zone (EASZ), and the Hellenic and Cyprus Arcs [38,39]. The convergence of the Arabian and Eurasian plates on the Bitlis-Zagros Suture causes the Anatolian Block to escape west between the EASZ and the NASZ. The pull effect (back-arc spreading) of the Hellenic Subduction Zone in western Anatolia hastens this escape [40–44].

Western Türkiye is characterized by rapid extension, making it one of the most dynamic regions on the continents. Consequently, this area exhibits high levels of seismic activity and its landscape is predominantly shaped by active normal faulting [45]. GNSS investigations point to a north–south regional extension in western Türkiye, which is termed the Western Anatolian Extensional Province (WAEP). This extension is occurring at a rate of roughly 30–40 mm per year [46–48].

The southern part of the WAEP is governed by E-W-trending horst–graben systems (e.g., Büyük Menderes, Küçük Menderes, Edremit, Simav, Gediz, and Gökova) and NW–SE-oriented active faults (e.g., Fethiye–Burdur Fault Zone). E–W-trending horst–graben systems are the most distinctive neotectonic characteristics of SW Türkiye, while NNW–SSE-trending basin-bounding faults are the other significant characteristic elements of this area [49–51].

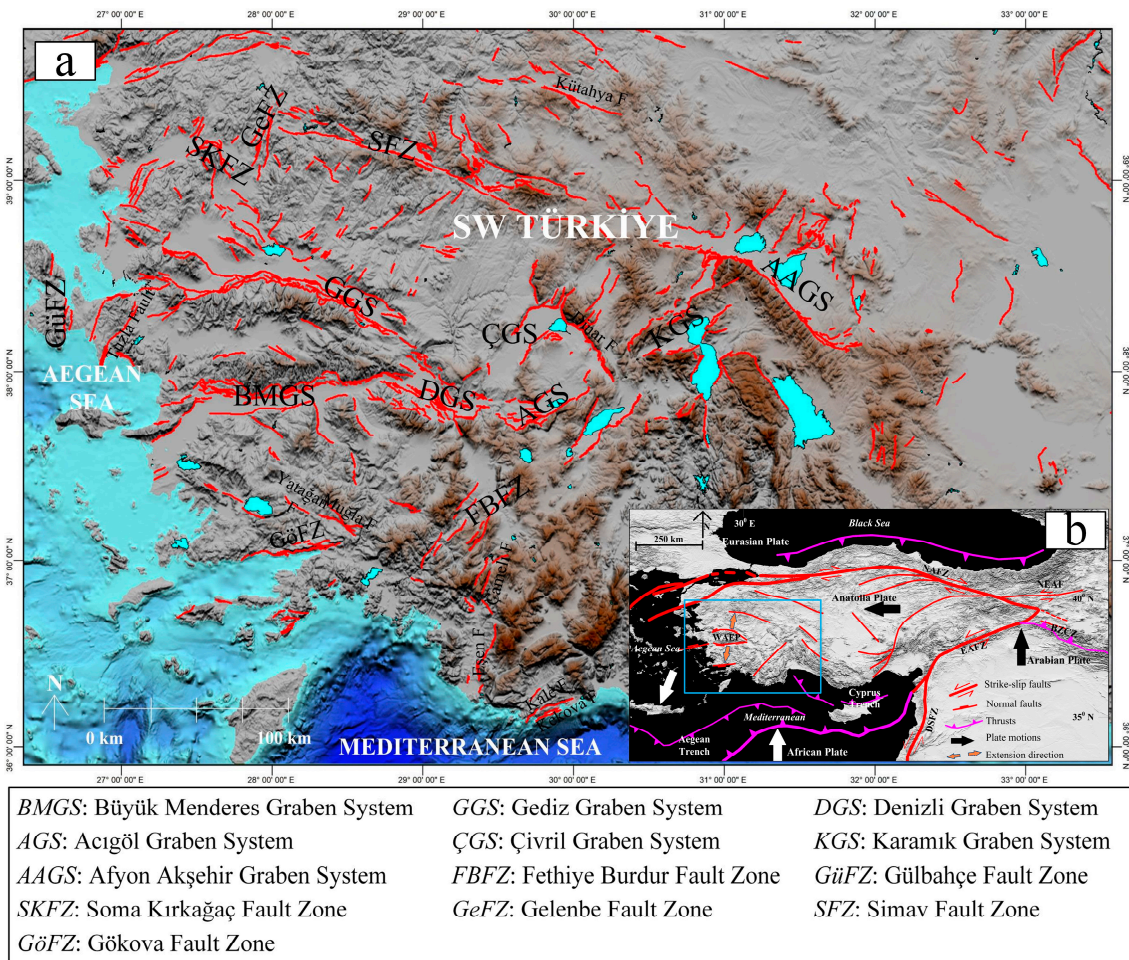


**Figure 2.** (a) Active tectonic structures located in SW Türkiye adopted from Emre et al. [52], (b) the main tectonic structures of Türkiye [53].

During the Miocene to Recent extension, two major tectonic structures, the Gediz Graben (GG) and the Büyük Menderes Graben (BMG), formed (Figure 3). Both grabens are 10–20 km wide and extend roughly 150 km inland from the Aegean coastline, having formed upon metamorphic rocks of the Menderes Massif [54]. The Menderes massif is a significant geological feature located in the southwestern region of Türkiye, encompassing an area of approximately 200 by 300 km<sup>2</sup>. It is characterized by a prominent assemblage of metamorphic rocks. The Menderes massif comprises three distinct submassifs, namely the northern, central, and southern submassifs, which are delineated by GG and BMG that extend in an east–west direction [55,56]. Along with the Menderes massif, two other important geological structures are the Bey Dağları platform and the west Anatolian Taurides. The west Anatolian Taurides, along with previously obducted ophiolites, exhibit overthrusting of the autochthonous Bey Dağları platform to the southeast. The Bey Dağları platform is composed of a carbonate platform spanning the Jurassic to Eocene periods, with some localized occurrences in the Oligocene epoch [57].

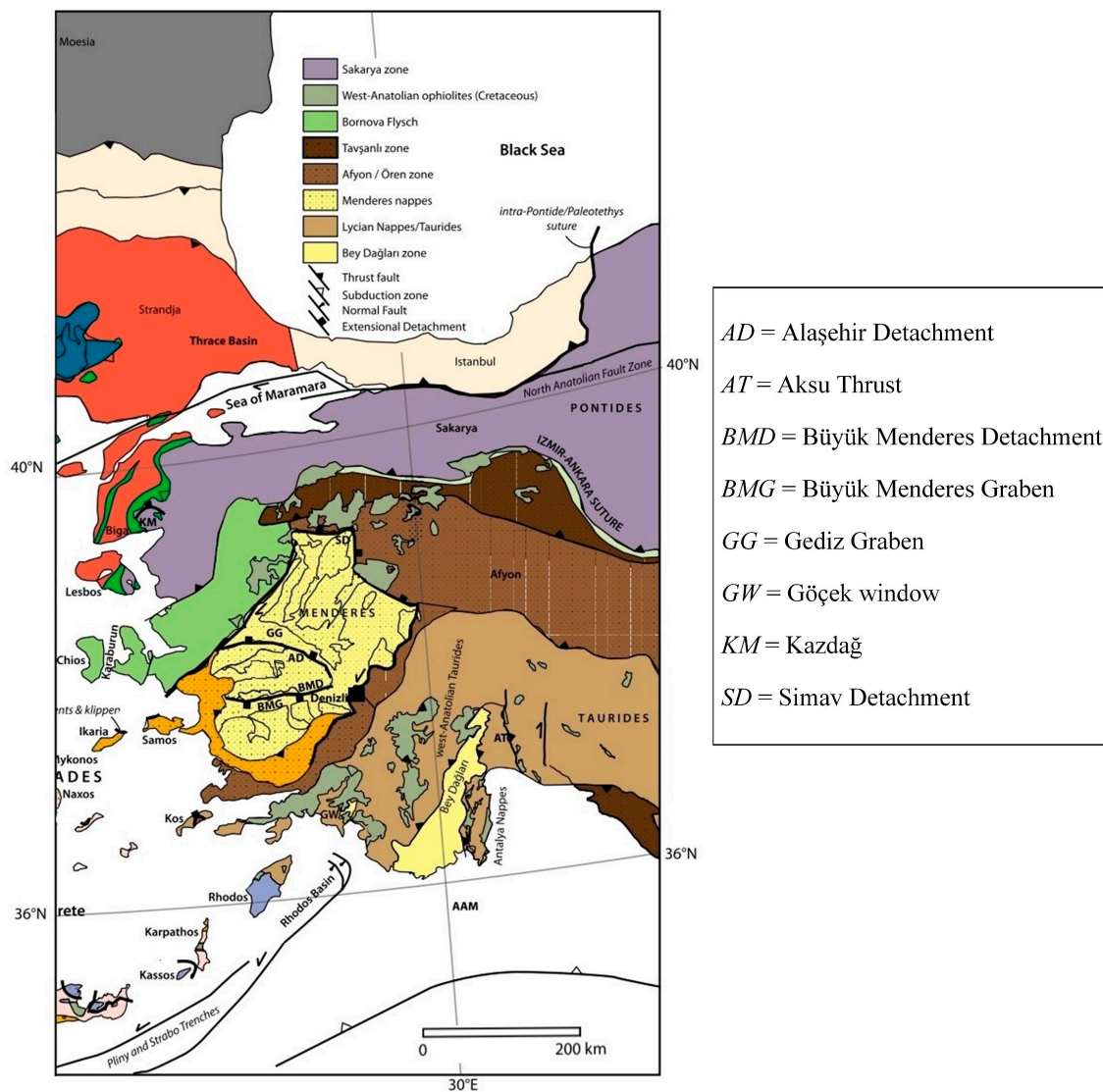


Figure 3. Geological map of the West Anatolian region [57].

There have been a number of historical and instrumental earthquakes in southwest Türkiye. These earthquakes destroyed many ancient cities in the region of SW Türkiye, which has a rich historical heritage, in addition to causing many deaths and the destruction of civilian structures. Ancient sites such as Kibyra, Patara, Lagina, and Stratonikeia were destroyed by the seismic activity in the region. The 1957 Fethiye earthquake was the cause of significant property damage and fatalities [58]. The significant earthquakes that have occurred in the study area are listed in Table 1.

Table 1. Significant earthquakes ( $M_w \geq 6.5$ ) of which took place in SW Türkiye [59].

| Date<br>(dd/mm/yyyy) | Latitude<br>(°N)<br>(WGS 84) | Longitude<br>(°E)<br>(WGS 84) | Magnitude<br>( $M_w$ ) | Date<br>(dd/mm/yyyy) | Latitude<br>(°N)<br>(WGS 84) | Longitude<br>(°E)<br>(WGS 84) | Magnitude<br>( $M_w$ ) |
|----------------------|------------------------------|-------------------------------|------------------------|----------------------|------------------------------|-------------------------------|------------------------|
| 30.10.2020           | 37.89                        | 26.71                         | 6.9                    | 22.4.1863            | 36.40                        | 27.60                         | 7.5                    |
| 20.7.2017            | 36.97                        | 27.41                         | 6.6                    | 3.11.1862            | 38.50                        | 27.71                         | 6.5                    |
| 9.10.1996            | 34.44                        | 32.13                         | 6.8                    | 2.12.1860            | 39.30                        | 29.70                         | 6.6                    |
| 25.4.1957            | 36.42                        | 28.68                         | 6.7                    | 28.2.1851            | 36.57                        | 29.21                         | 6.8                    |
| 24.4.1957            | 36.43                        | 28.63                         | 6.5                    | 23.6.1845            | 38.60                        | 27.50                         | 6.7                    |
| 16.7.1955            | 37.65                        | 27.26                         | 6.5                    | 3.7.1778             | 38.42                        | 27.14                         | 6.5                    |

Table 1. Cont.

| Date<br>(dd/mm/yyyy) | Latitude<br>(°N)<br>(WGS 84) | Longitude<br>(°E)<br>(WGS 84) | Magnitude<br>( $M_w$ ) | Date<br>(dd/mm/yyyy) | Latitude<br>(°N)<br>(WGS 84) | Longitude<br>(°E)<br>(WGS 84) | Magnitude<br>( $M_w$ ) |
|----------------------|------------------------------|-------------------------------|------------------------|----------------------|------------------------------|-------------------------------|------------------------|
| 9.2.1948             | 35.41                        | 27.20                         | 6.8                    | 1.9.1771             | 38.44                        | 27.59                         | 6.6                    |
| 6.10.1944            | 39.48                        | 26.56                         | 6.5                    | 13.2.1756            | 36.30                        | 27.50                         | 7.5                    |
| 26.6.1926            | 36.54                        | 27.33                         | 7.2                    | 24.2.1755            | 39.10                        | 26.55                         | 6.8                    |
| 18.3.1926            | 35.84                        | 29.50                         | 6.5                    | 18.6.1751            | 37.71                        | 27.01                         | 6.7                    |
| 18.03.1926           | 35.99                        | 30.13                         | 6.7                    | 31.1.1741            | 36.16                        | 28.50                         | 7.5                    |
| 13.08.1922           | 35.51                        | 27.98                         | 6.6                    | 4.4.1739             | 38.58                        | 26.89                         | 6.8                    |
| 3.10.1914            | 37.70                        | 30.40                         | 6.6                    | 25.2.1702            | 37.78                        | 29.08                         | 6.8                    |
| 20.9.1899            | 37.88                        | 28.08                         | 6.7                    | 10.7.1688            | 38.37                        | 27.13                         | 6.8                    |
| 29.1.1898            | 39.42                        | 28.06                         | 6.9                    | 10.9.1688            | 39.65                        | 27.88                         | 6.6                    |
| 19.8.1895            | 37.87                        | 27.93                         | 6.5                    | 22.2.1653            | 37.88                        | 28.17                         | 6.7                    |
| 15.10.1883           | 38.30                        | 26.43                         | 6.7                    | 00.00.1609           | 36.20                        | 29.00                         | 7.2                    |
| 13.5.1876            | 38.80                        | 30.50                         | 6.8                    | 00.00.1528           | 39.10                        | 26.55                         | 6.9                    |
| 3.5.1875             | 38.10                        | 30.10                         | 6.8                    | 18.10.1493           | 36.65                        | 27.21                         | 6.9                    |
| 16.11.1874           | 36.50                        | 27.90                         | 7.0                    | 20.3.1389            | 38.26                        | 26.54                         | 6.6                    |
| 18.4.1869            | 36.50                        | 27.60                         | 6.8                    | 6.8.1384             | 39.10                        | 26.55                         | 6.6                    |
| 1.12.1869            | 37.03                        | 28.33                         | 6.8                    | 30.4.1366            | 36.43                        | 28.23                         | 6.7                    |
| 7.3.1867             | 39.24                        | 26.26                         | 6.8                    | 17.7.1296            | 39.09                        | 27.43                         | 6.9                    |
| 23.7.1865            | 39.43                        | 26.25                         | 6.6                    | 2.2.1040             | 38.42                        | 27.14                         | 6.5                    |

### 3. Probabilistic Seismic Hazard Assessment (PSHA) for SW Türkiye Region and Developing Site-Specific Earthquake Spectra for the Cities

The technique of PSHA considers various seismic factors that could impact a given area to evaluate the frequency at which specific levels of ground motion are surpassed. In order to evaluate the seismicity of the area in PSHA, it is necessary to compute the earthquake distribution and recurrence relationships for the region [60,61].

The precise determination of the location, magnitude, and temporal occurrence of forthcoming earthquakes remains uncertain. Numerous stochastic models have been developed to depict the probabilistic distribution of earthquakes over time. Using a probabilistic method, the seismic hazard for cities in southwestern Türkiye was assessed as part of this research. For this purpose, a new database of shallow crustal earthquakes from 1000 to 2023 was produced based on a unified moment magnitude scale. Depending on the space–time windows, foreshock and aftershock occurrences in the catalog were removed, and a catalog completeness analysis was undertaken. The epicentral distribution of the earthquakes in the study region is depicted in Figure 4. Uncertainty in determining magnitude was considered in the study. Seismic sources were characterized as homogenous area source zones, taking active fault zones into account. The seismic hazard analysis for SW Türkiye performed in this study utilized the conventional probabilistic methodology proposed by Cornell [62]. Using the Kijko–Smit [63] maximum likelihood estimation approach, the activity rate ( $\lambda$ ) and the Gutenberg–Richter “ $b$ ” parameter as earthquake hazard parameters were assessed for every seismic source.

An “efficacy test” employing the average log likelihood value (LLH) was conducted to identify the best appropriate ground motion prediction equations (GMPEs) for southwestern Türkiye. Based on the regional rupture characteristics [64] and the Kijko–Sellevoll [65] methodology, the maximum magnitude ( $M_{max}$ ) of each seismic source was estimated. Using geographical information system (GIS) software (ArcGIS Pro v.3.1.1) seismic hazard maps for southwestern Türkiye for PGA, spectral acceleration (SA) with periods of 0.2 and 1 sec, and for bedrock with a hazard level of 10% probability of exceedance in 50 years were created. As part of the research, site-specific seismic hazard curves and uniform hazard spectra (UHS) were developed for the urban areas of southwestern Türkiye (Figure 5).

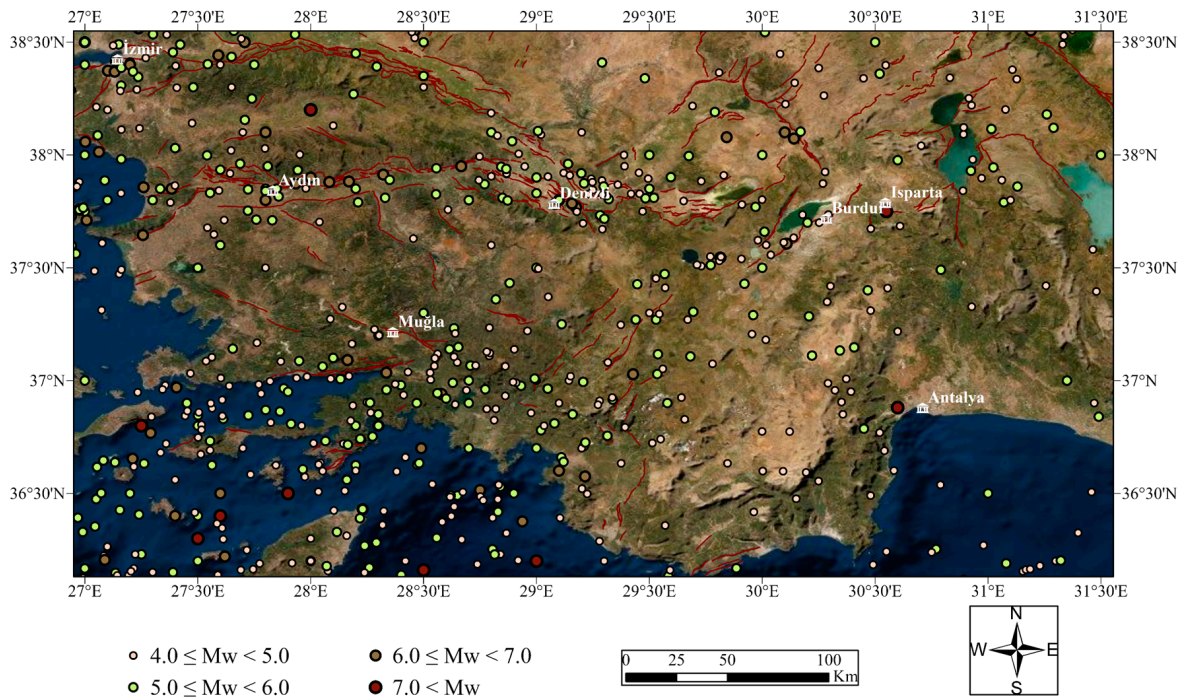


Figure 4. The distribution of shallow crustal earthquakes in SW Türkiye.

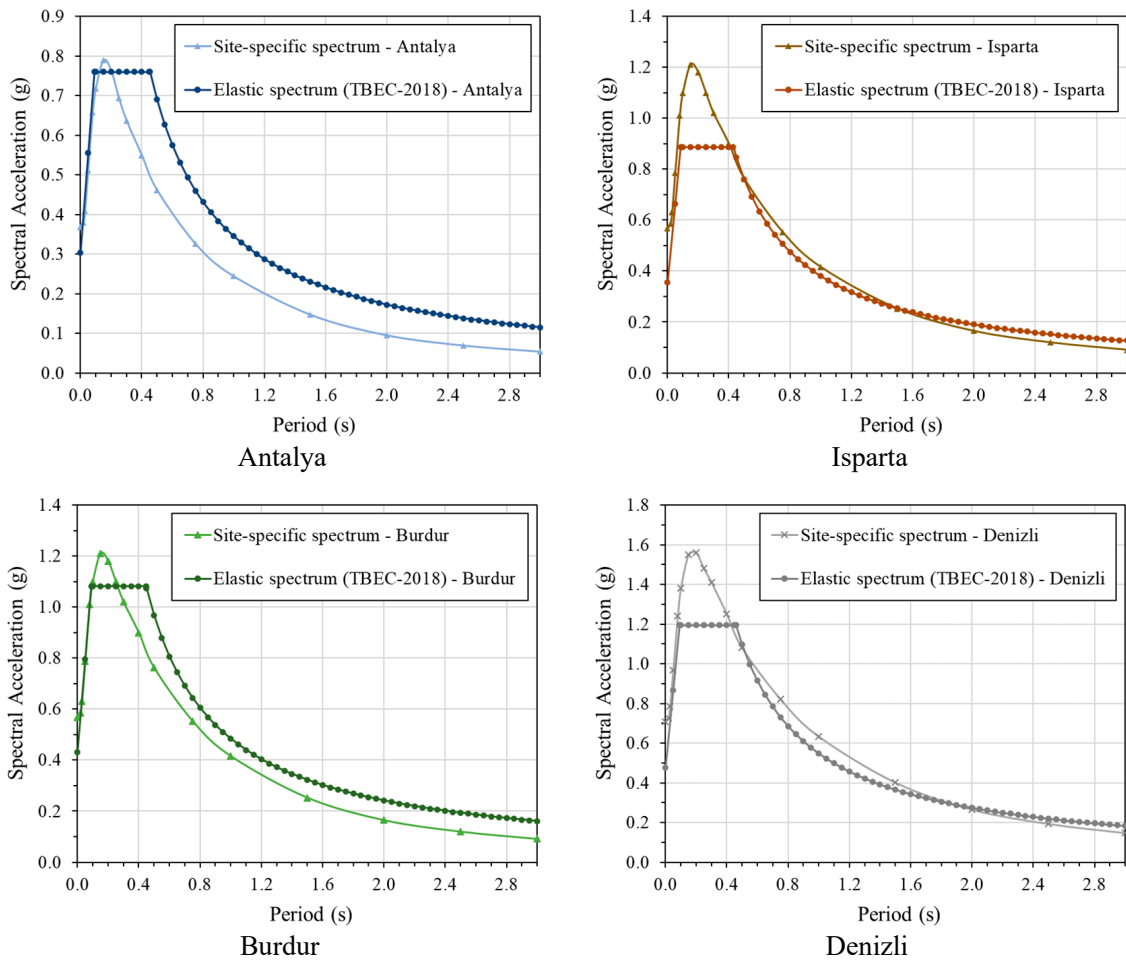
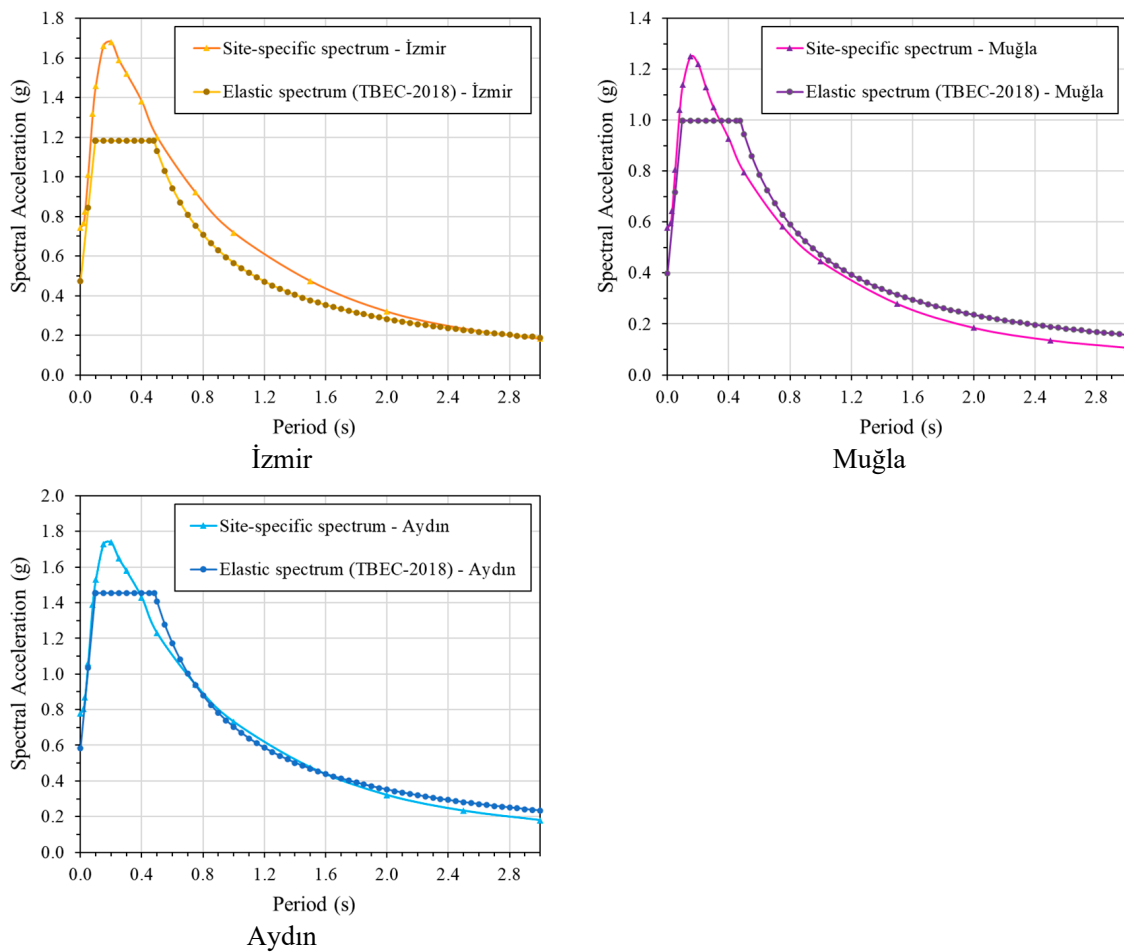


Figure 5. Cont.



**Figure 5.** The developed site-specific uniform hazard response spectra for 10% probability of exceedance in 50 years and for ZD sites with 5% damping for the provinces and comparisons with TBEC-2018 elastic spectra.

The seismic hazard curves were created for the urban areas of Antalya, Isparta, Burdur, Denizli, İzmir, Muğla, and Aydın located in the southwestern region of Türkiye. The curves obtained depict the annual frequency of exceeding certain levels of peak ground acceleration (PGA) and spectral accelerations at periods of  $T = 0.2$  and  $T = 1.0$  s specifically for ZD sites. The hazard curves presented in Figure 6 incorporate the combined effects of all seismic sources within the region. The municipalities of Aydın, İzmir, and Denizli have been shown to possess notably heightened levels of seismic hazard and demonstrate relatively greater vulnerability to seismic risk in comparison to other municipalities in the region.

Figure 6 displays the resulting hazard curves, which take into consideration the contributions of all seismic sources in the region. It has been determined that the municipalities of Aydın, İzmir, and Denizli exhibit significantly elevated levels of seismic hazard and are comparatively more susceptible to seismic risk when compared to other municipalities within the region.

The reason for the spectrum differences is the different methods used in the analyses in this study and TBEC-2018. While preparing TBEC-2018, the Weichert [66] method was preferred in calculating earthquake magnitude recurrence parameters. “ $b$ ” values calculated with the Weichert method were used to create recurrence models of seismic sources. In this study, the Kijko–Smit method was preferred to calculate earthquake magnitude recurrence parameters. In this method, the main catalog is divided into subcatalogs according to their completion periods, and the  $b$  and  $\lambda$  values calculated for each subcatalog are combined, taking into account the number of earthquakes in each subcatalog and their completion times. The cumulative visual inspection (CUVI) method, developed by Tinti

and Mulargia [67], was used in this study to determine the complete parts of the catalog.  $b$  and  $\lambda$  values calculated using the Matlab code prepared by Kijko [68] were used to create recurrence models of seismic sources. Another difference is that the maximum magnitude ( $M_{max}$ ) of each seismic source was calculated based on the unique regional rupture characteristics, and Kijko–Sellevoll used statistical methods. As a result of a detailed examination of the earthquakes that occurred in SW Türkiye, the ground motion prediction equations that provided the best prediction for the region were selected. The equations used in this study are different from TBEC-2018.

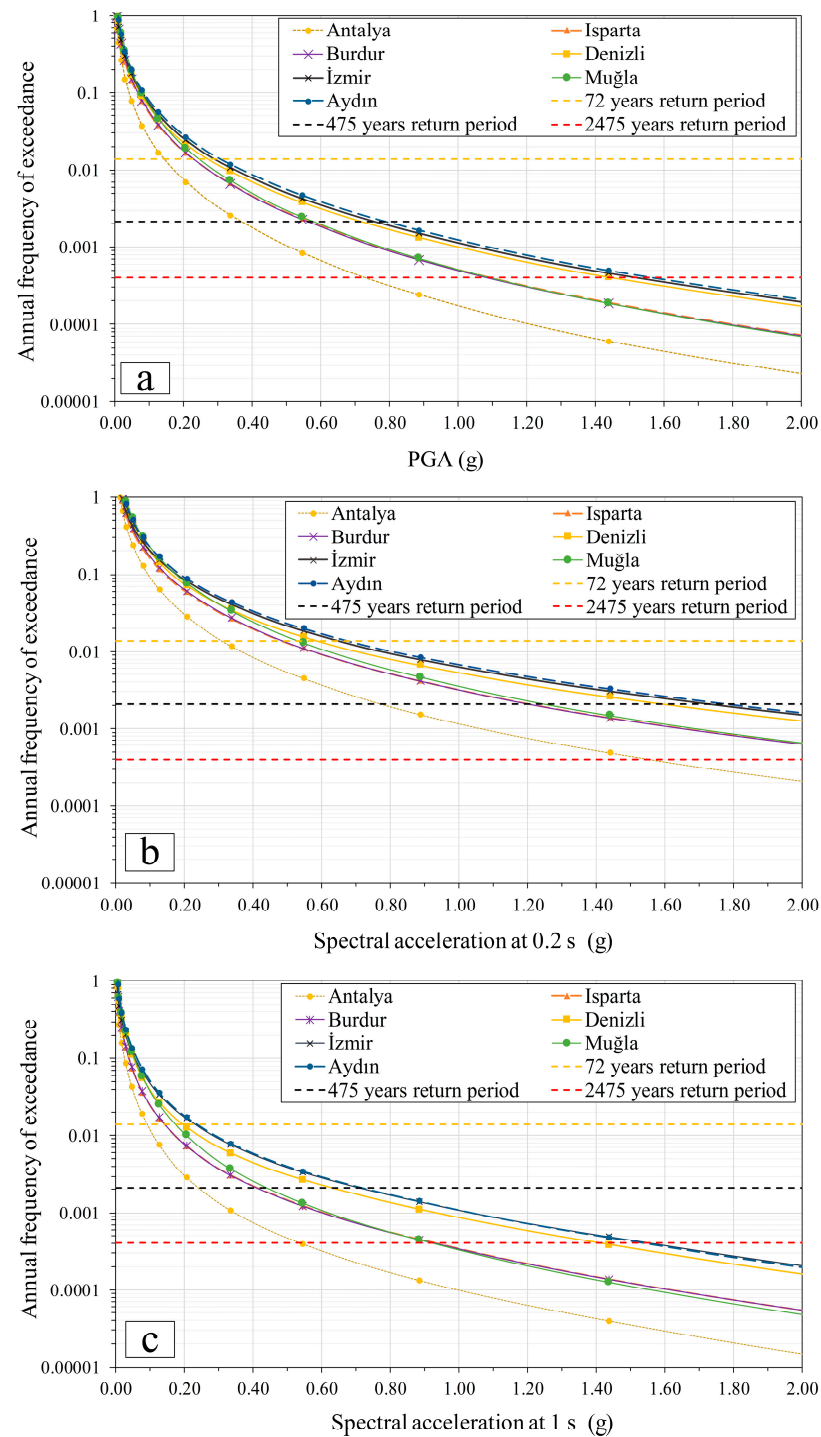


**Figure 6.** The developed seismic hazard curves for (a) PGA, (b)  $T = 0.2$  s, and (c)  $T = 1$  s spectral periods for ZD sites for the provinces.

#### 4. Structural Analyses

In TBEC-2018, building performance levels are defined for building structural systems under earthquake effects as the basis for the definition of building performance targets. These are continuous use performance level (CUPL), limited damage performance level (LDPL), controlled damage performance level (CDPL), and collapse prevention performance level (CPPL). Buildings that cannot provide any of the four performance levels are in Collapse Condition (CC). The performance level of the building is determined by the conditions given in Table 2 by considering the damage zones where the elements are located.

**Table 2.** Conditions to be met by structural elements according to performance level.

| Performance Level | Structural Element Type  | Condition  |
|-------------------|--|--|
| CUPL              | Beam   | All beams are in the limited damage zone.  |
|                   | Column   | All columns are in the limited damage zone.  |
| LDPL              | Beam   | Maximum of 20% of the beams in the direction of calculation may pass into the significant damage zone.   |
|                   | Column   | All columns are in the limited damage zone.  |
| CDPL              | Beam   | Maximum of 35% of the beams in the direction of calculation may pass into the significant damage zone.   |
|                   | Column   | The ratio of the sum of the shear forces of the vertical elements in the advanced damage zone at each floor to the sum of the shear forces of all vertical elements at that floor should be less than 20%. At the top story, this ratio can be at maximum 40%. |
|                   |  | The ratio of the shear forces carried by the vertical members whose upper and lower sections both exceed the significant damage limit at any story to the ratio of the shear forces carried by all vertical members at that story should not exceed 30%.       |
|                   |  | There should be no column passing into the collapse zone.  |
| Beam              | In the calculation direction, a maximum of 20% of the beams may pass into the collapse zone. |  |
| CPPL              | Column   | The ratio of the shear forces carried by the vertical members whose upper and lower sections both exceed the significant damage limit at any story to the ratio of the shear forces carried by all vertical members at that story should not exceed 30%.       |
|                   |  | There should be no column passing into the collapse zone.  |

At the cross-section level, TBEC-2018 sets out three damage states and damage limits for ductile elements. These are limited damage (LD), controlled damage (CD), and pre-collapse damage (PCD) and their limit values. Elements whose critical section damage does not reach LD are in the limited damage zone (LDZ), elements between LD and CD are in the significant damage zone (SDZ), elements between CD and PCD are in the advanced damage zone (ADZ), and elements exceeding PCD are in the collapse zone (CZ) (Figure 7).

Cross-section damage is determined by comparing the deformations occurring in the sections as a result of the nonlinear analysis with the unit strain upper limits given in Table 3. Brittle damaged elements are not included in the conditions given in Table 3. Brittle damaged elements need to be strengthened.

If the earthquake safety of the building is to be determined by using one of the static pushover methods, the roof story of the building should be pushed up to the target displacement level. Thus, the amount of plastic rotation that will occur in the structural element cross-sections is determined. In order to obtain the target displacement level, the intersection of the modal capacity spectrum and the spectrum curve is required. The modal capacity spectrum is obtained by axis transformation of the capacity curve obtained as a result of pushover analysis. With axis transformation, the modal capacity curve whose axes

are spectral acceleration ( $S_a$ )–spectral displacement ( $S_d$ ) is obtained from the capacity curve whose axes are base shear force–displacement. The purpose of the axis transformation is to bring the capacity curve and spectrum curve together on the same graph. Plotting the modal capacity curve and spectrum curve on the same graph is shown in Figure 8. The target displacement is obtained by multiplying the modal participation multiplier by the modal displacement demand ( $d_i^{(p)}$ ) obtained in Figure 8. According to TBEC-2018, the elastic spectrum to be used in determining the earthquake safety of buildings under the earthquake effect is created according to a 5% damping ratio.

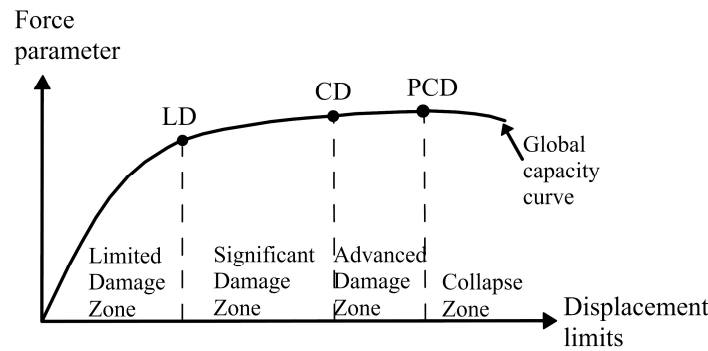


Figure 7. Section damage limits and damage zones (TBEC-2018).

Table 3. Upper limits of allowable strain according to section damage limits.

| Section Damage Limit | Plastic Rotation Upper Limits ( $\theta_p$ )  |
|----------------------|---|
| PCD                  | $\theta_p^{(PCD)} = \frac{2}{3} \left( (\phi_u - \phi_y) L_p \left( 1 - 0.5 \frac{L_p}{L_s} \right) + 4.5 \phi_u d_b \right)$ |
| CD                   | $\theta_p^{(CD)} = 0.75 \theta_p^{(PCD)}$   |
| LD                   | $\theta_p^{(LD)} = 0$   |

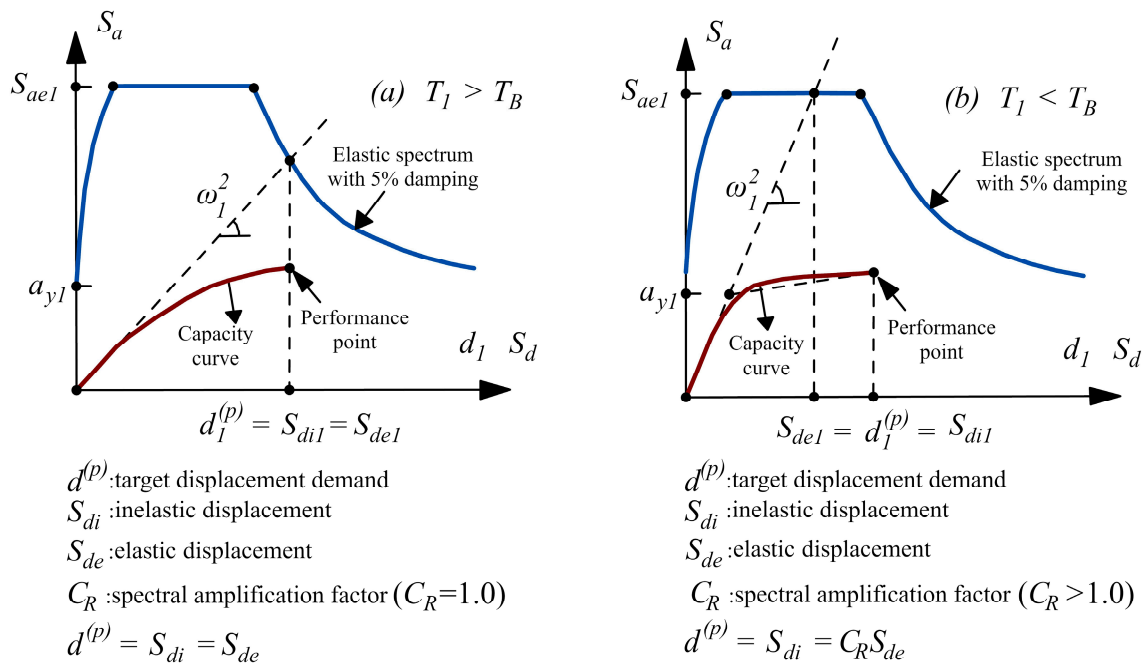
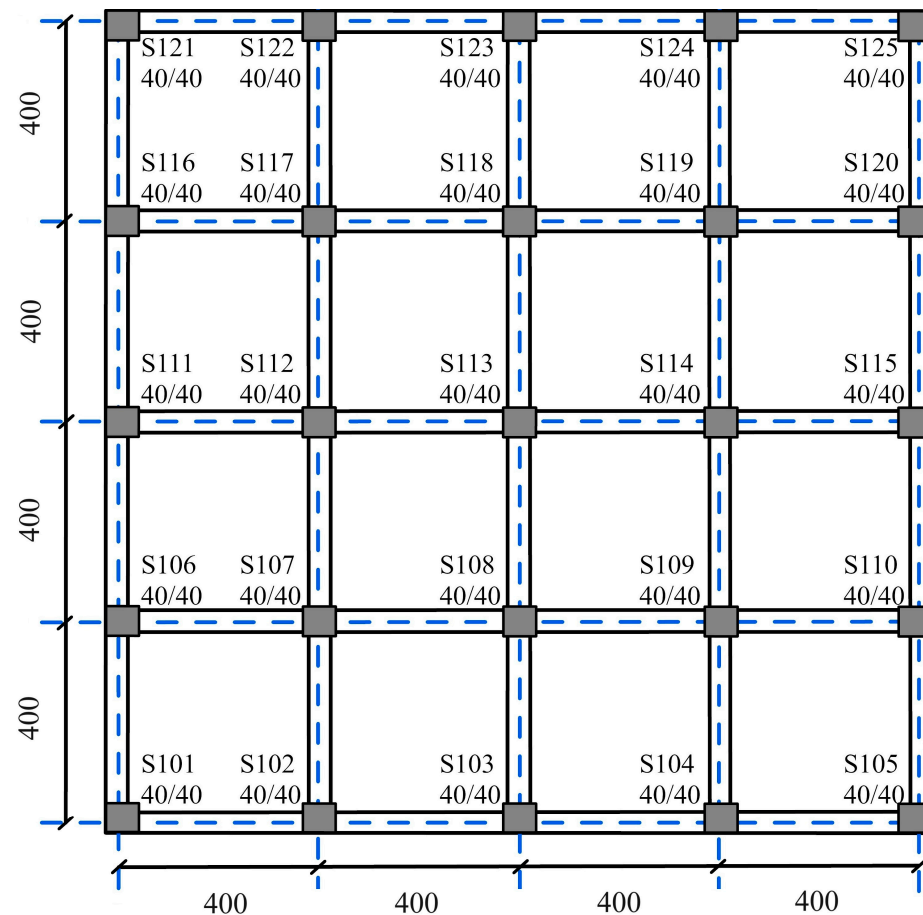


Figure 8. Modal capacity curve and elastic spectrum for (a) flexible structures (b) rigid structures shown on the same graph [69].

The use of a site-specific spectrum instead of the elastic spectrum given in TBEC-2018 may cause the target displacement level of the building to change. In this study, the effect of this change on the earthquake safety of buildings used for residential purposes in the southwestern Anatolia region of Türkiye was investigated. For this purpose, the model building with the formwork plan given in Figure 9 was selected.



**Figure 9.** The formwork plan of the RC building selected as an example (units in cm).

The model building selected as an example was modeled with a height of 3 m for each floor and a total of 5 floors. C15 concrete and B420C reinforcement class are used in all structural elements of the building to represent the existing medium-quality buildings in the region. The slab dead load ( $g$ ) and live load ( $q$ ) of the building were taken as  $4.5 \text{ kN/m}^2$  and  $2 \text{ kN/m}^2$ , respectively. The purpose of use of the building is residential, and the cross-sections of the structural elements of the building are given in Figure 10. The structural system and material properties of the building (concrete and reinforcement class, number of stories, structural system properties, etc.) were selected to represent the majority of the existing building stock in the study region.

Static pushover analysis of the selected model building was performed in the SAP2000 [70] program. The plastic hinge properties of the sections used in the analysis were determined by moment curvature analysis performed in the section designer interface of the SAP2000 program. A lumped plastic hinge model was used as the nonlinear behavior model of columns and beams. The length of the plastic deformation zone ( $L_p$ ), called the plastic hinge length, was taken as equal to half of the section dimension in the calculation direction. Plastic hinges are assigned to both ends of the columns and beams. The building capacity curve was obtained by static pushover analysis.

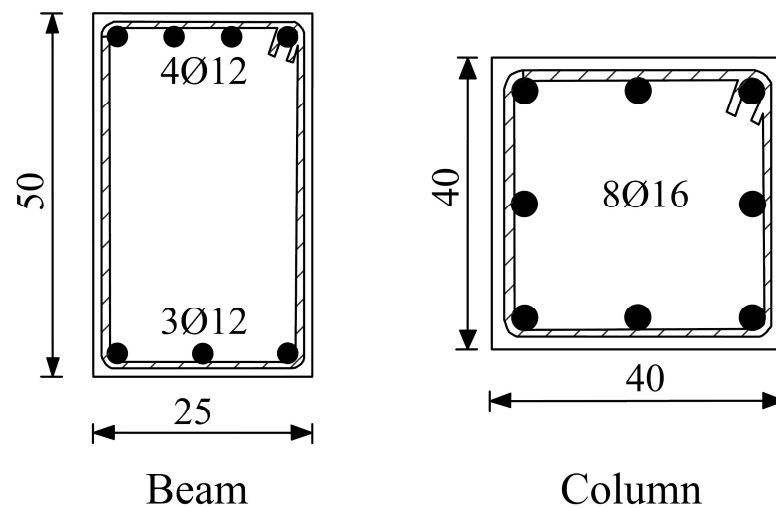


**Figure 10.** Beam and column cross-sections (unit of cross-sectional dimensions in cm).

The minimum target performance level of reinforced concrete buildings differs according to the purpose of use of the building. According to TBEC-2018, residential buildings must meet the target performance level of controlled damage performance level (CDPL) for earthquakes with a return period of 475 years. Therefore, the spectrum to be used in determining the target displacement of the building should be the spectrum determined for earthquakes with a return period of 475 years. The determination of the target displacements for each province according to both the TBEC-2018 and the site-spectrum curves obtained on a province basis is given in Figure 11 on the same graph. The slope of the initial tangent shown in green in the graphs was calculated as the square of the dominant angular frequency of the model building ( $\omega^2$ ). The initial tangent drawn from the modal capacity curve is intersected by both spectrum curves. Thus, the modal displacement according to TBEC-2018 ( $d_{TBEC-2018}^{(p)}$ ) and the modal displacement according to the site-specific spectrum ( $d_{site-specific}^{(p)}$ ) were found for each province separately (Figure 11).

Target displacements were obtained by multiplying the modal participation multiplier and the modal displacement demands ( $d_{site-specific}^{(p)}$ ,  $d_{TBEC-2018}^{(p)}$ ) obtained in Figure 11. The target displacement values obtained for both spectra for all cities are shown in Figure 12 and compared with each other.

When Figure 12 is analyzed, it is seen that the target displacements obtained by using the site-specific spectra in Isparta, Denizli, İzmir, and Aydın provinces are higher than the target displacements obtained according to TBEC-2018. This shows that the deformations (plastic rotation) that will occur in the structural elements as a result of the pushover analysis to be performed with the site-specific spectra obtained for these provinces will be higher than for TBEC-2018. In Antalya, Burdur, and Muğla, it is seen that the target displacements obtained according to TBEC-2018 are higher than the target displacements obtained by using the site-specific spectra obtained for the provinces. This situation shows that the deformations (plastic rotation) that will occur in the structural elements as a result of the pushover analysis to be performed with the site-specific spectra obtained for these provinces will be less than for TBEC-2018.

The model building was subjected to static pushover analysis up to the target displacement values obtained according to both TBEC-2018 and site-specific spectra for each province within the scope of the study, and the damage occurring in the structural elements was obtained (Figure 13). The pink-colored plastic hinge in the structural elements in this figure shows that the damage in the cross-section remains in the limited damage zone (LDZ), the blue-colored plastic hinge shows that the damage in the cross-section remains in the significant damage zone (SDZ), the turquoise-colored plastic hinge shows that the damage in the cross-section remains in the advanced damage zone (ADZ), and the green-

colored plastic hinge shows that the damage in the cross-section remains in the collapse zone (CZ).

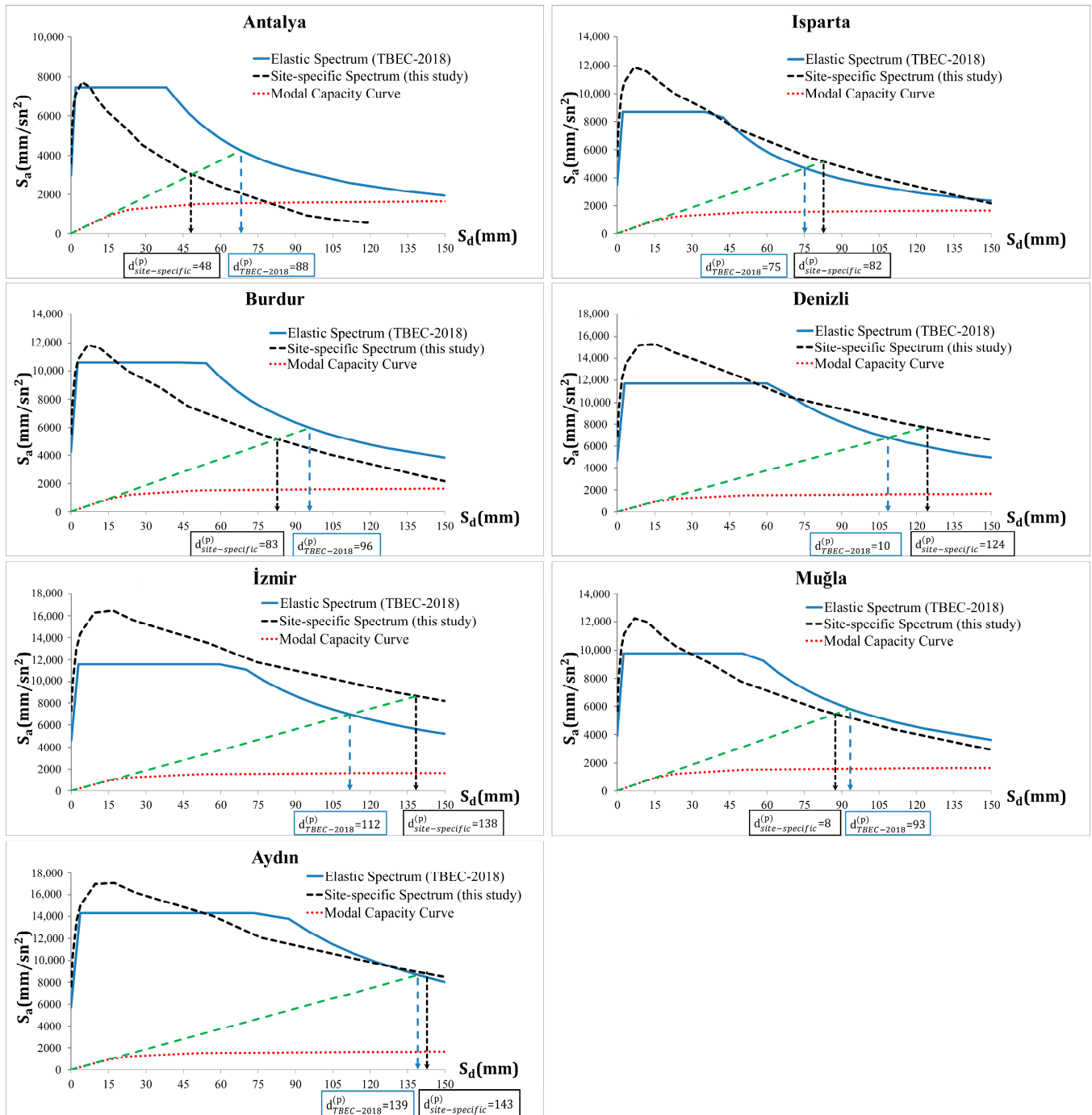


**Figure 11.** Determination of target displacement demands for the provinces according to both TBEC-2018 and site-specific earthquake spectra.

When the performance analyses were performed according to the site-specific spectra instead of the elastic spectrum given in TBEC-2018, it caused the damage zone of some structural elements to change. The number of structural elements with changed damage zone is given in Figure 14.

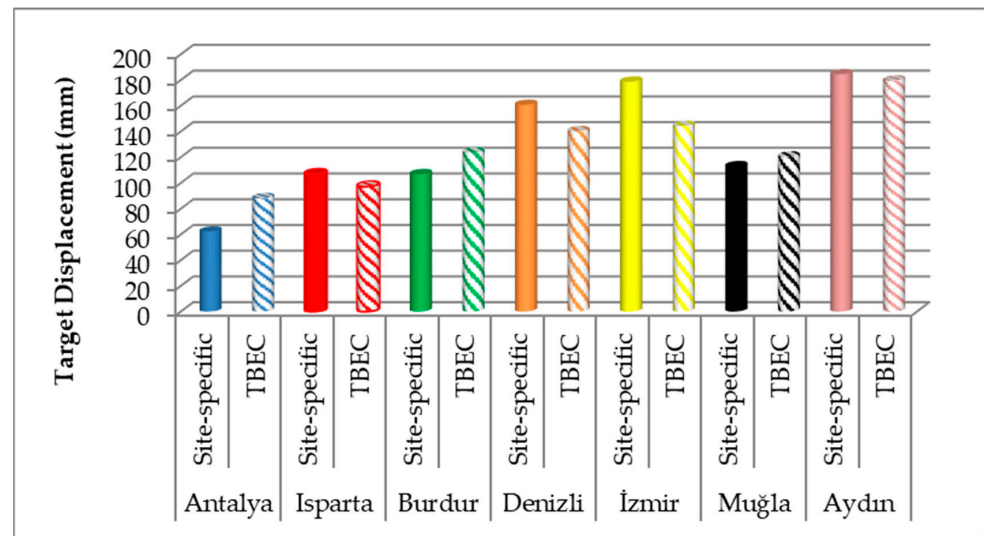


Figure 12. Comparison of target displacement values for the provinces.

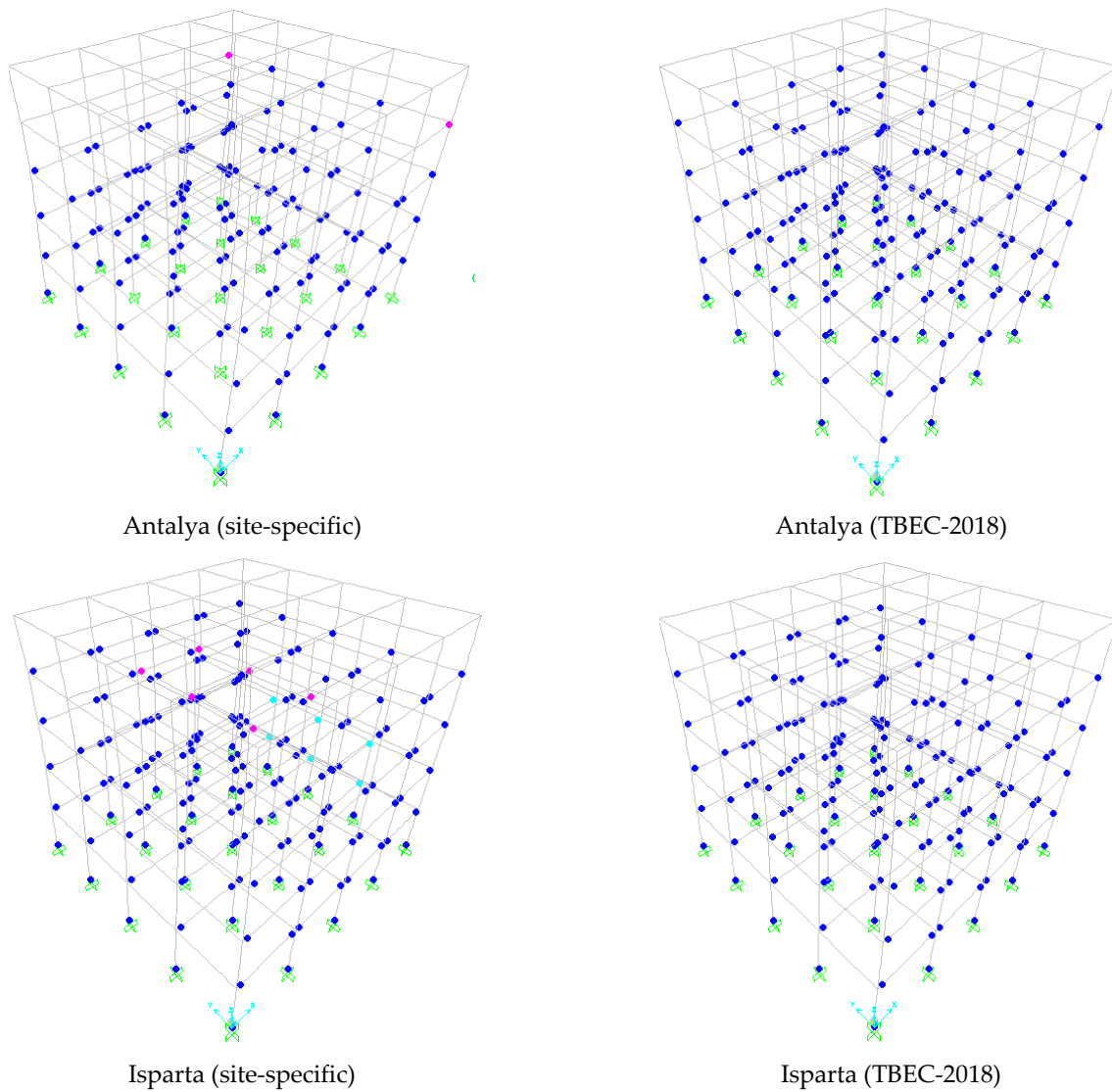


Figure 13. Cont.

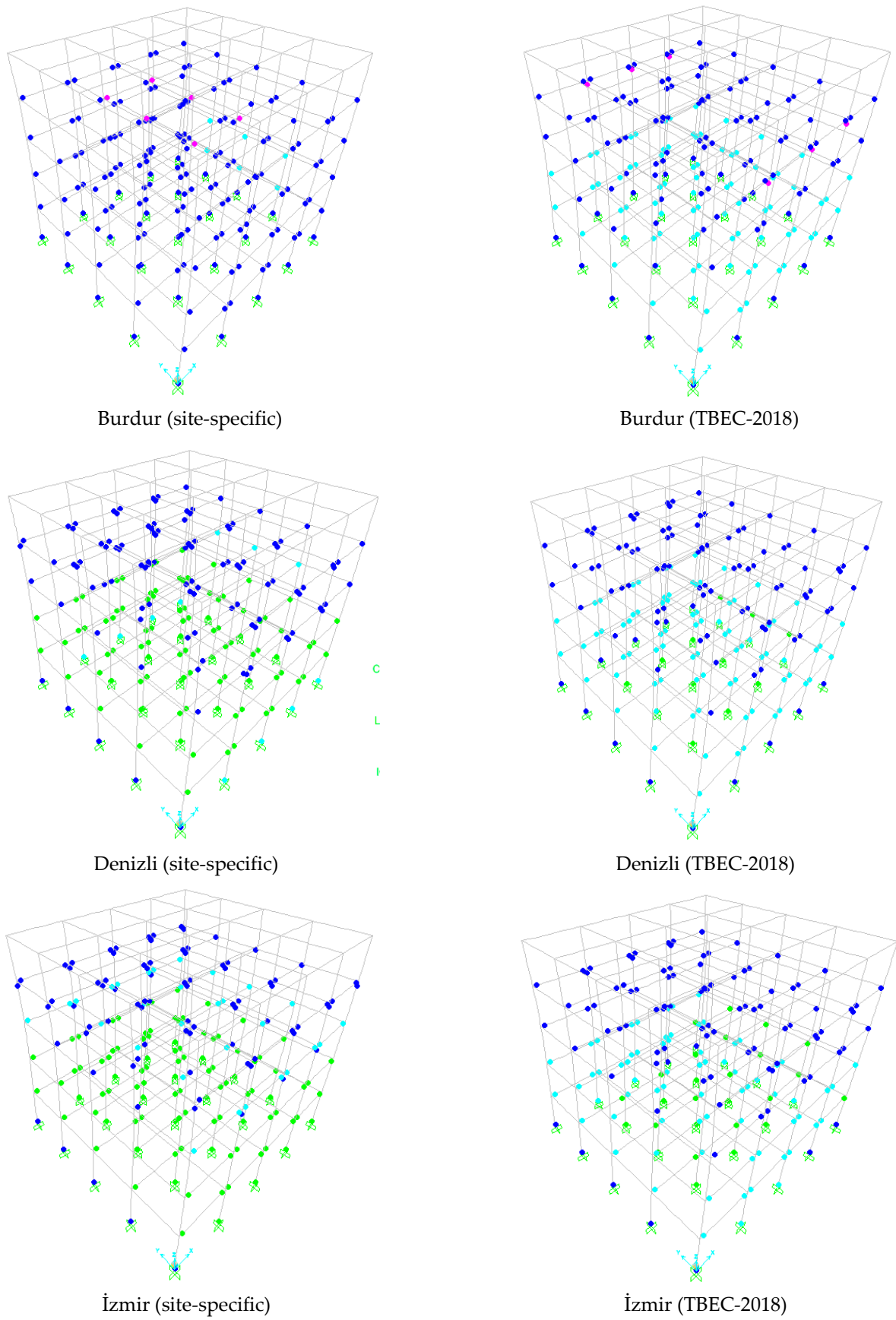
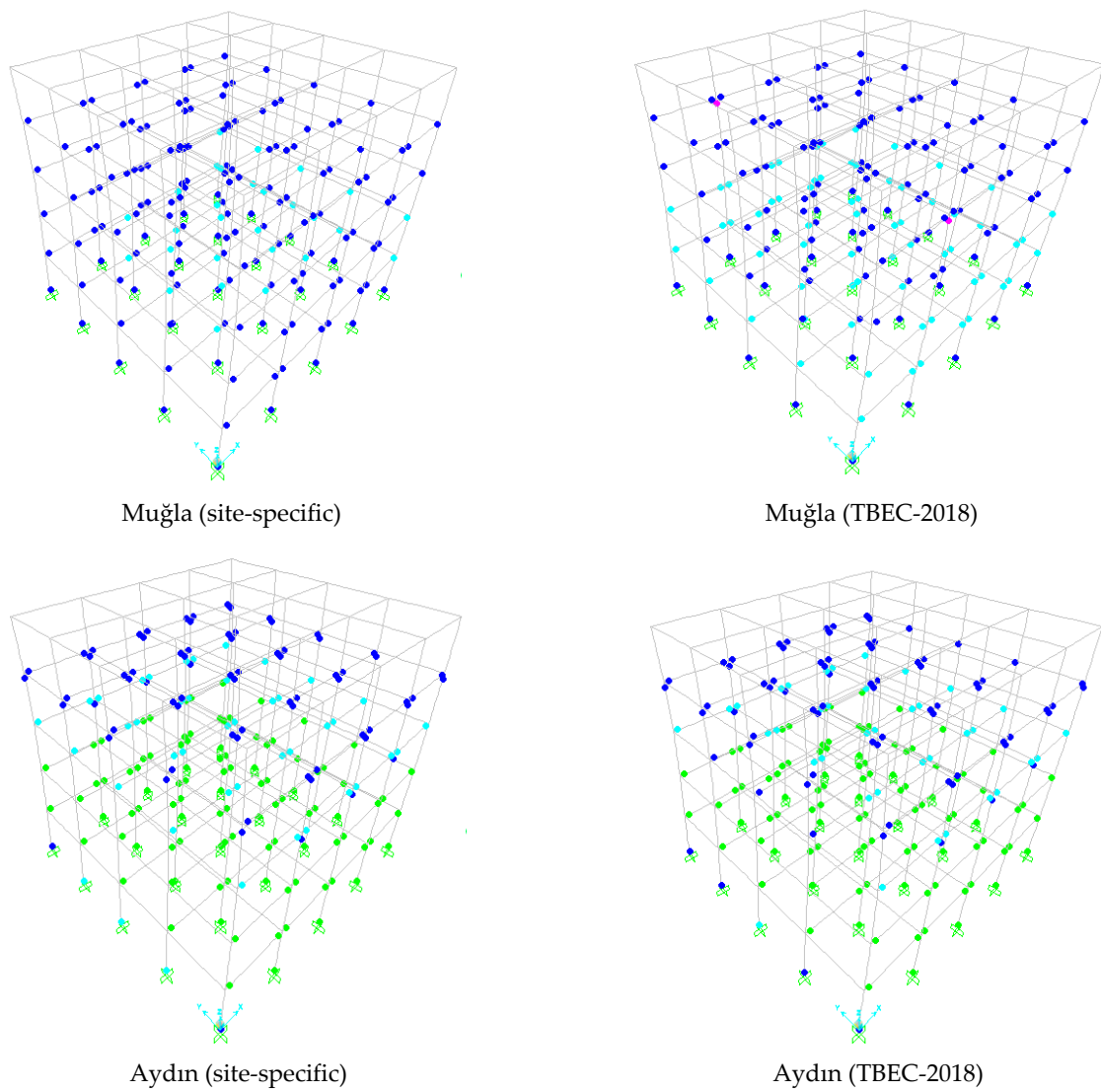
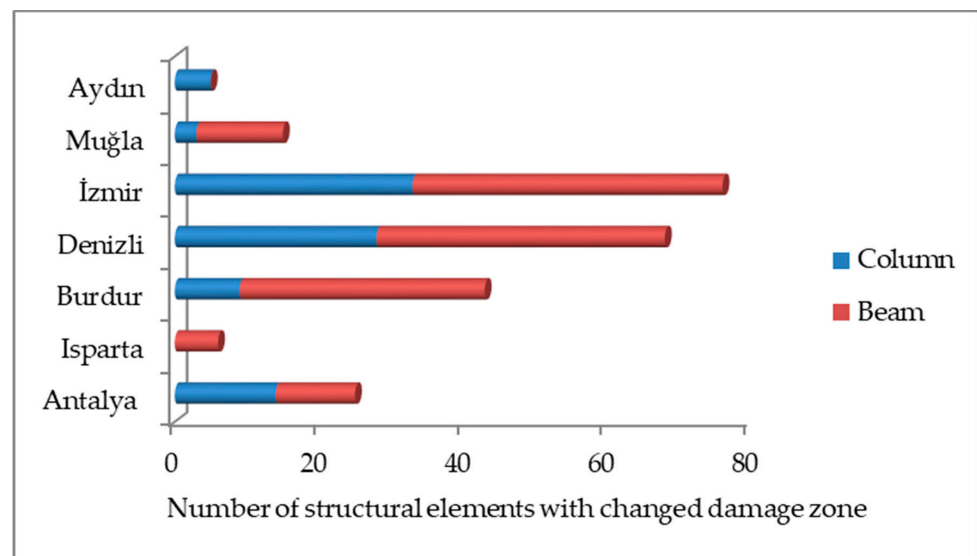


Figure 13. Cont.



**Figure 13.** Comparison of structural element damage for the provinces.



**Figure 14.** Number of structural elements with changed damage zone for the provinces.

Figure 14 shows that the number of structural elements whose damage zone changed due to spectrum change was the highest in İzmir and the lowest in Aydın. Damage zones of 33 columns and 43 beams changed due to spectrum changes in İzmir.

In order to examine the effect of structural element damage zone change on the performance level of the floors and the building, the performance level of each floor of the model building and the performance level of the building were determined separately for all provinces according to both spectra. The most unfavorable performance level among the performance levels of the floors was determined as the building performance level. The performance levels obtained for the floors and the building according to the damage occurring only in the beams (considering the conditions given in Table 2 regarding only the beams) are given in Table 4. The floors whose performance level changed due to spectrum changes are shown in italic red.

**Table 4.** Comparison of performance levels according to the damage to beams.

| Province | Used Spectrum Curve | Floor Performance Levels |             |             |          |          | Building Performance Level |
|----------|---------------------|--------------------------|-------------|-------------|----------|----------|----------------------------|
|          |                     | 1. Floor                 | 2. Floor    | 3. Floor    | 4. Floor | 5. Floor |                            |
| Antalya  | Site-specific       | CDPL                     | CDPL        | CDPL        | CDPL     | LDPL     | CDPL                       |
|          | TBEC-2018           | CDPL                     | CDPL        | CDPL        | CDPL     | LDPL     | CDPL                       |
| Isparta  | Site-specific       | CDPL                     | CDPL        | CDPL        | CDPL     | LDPL     | CDPL                       |
|          | TBEC-2018           | CDPL                     | CDPL        | CDPL        | CDPL     | LDPL     | CDPL                       |
| Burdur   | Site-specific       | <b>CDPL</b>              | <b>CDPL</b> | CDPL        | CDPL     | LDPL     | <b>CDPL</b>                |
|          | TBEC-2018           | <b>CPPL</b>              | <b>CPPL</b> | CDPL        | CDPL     | LDPL     | <b>CPPL</b>                |
| Denizli  | Site-specific       | <b>CC</b>                | <b>CC</b>   | CDPL        | CDPL     | LDPL     | <b>CC</b>                  |
|          | TBEC-2018           | <b>CPPL</b>              | <b>CPPL</b> | CDPL        | CDPL     | LDPL     | <b>CPPL</b>                |
| İzmir    | Site-specific       | <b>CC</b>                | <b>CC</b>   | <b>CPPL</b> | CDPL     | LDPL     | <b>CC</b>                  |
|          | TBEC-2018           | <b>CC</b>                | <b>CPPL</b> | <b>CDPL</b> | CDPL     | LDPL     | <b>CPPL</b>                |
| Muğla    | Site-specific       | CPPL                     | CPPL        | CDPL        | CDPL     | LDPL     | CPPL                       |
|          | TBEC-2018           | CPPL                     | CPPL        | CDPL        | CDPL     | LDPL     | CPPL                       |
| Aydın    | Site-specific       | CC                       | CC          | CPPL        | CDPL     | LDPL     | CC                         |
|          | TBEC-2018           | CC                       | CC          | CPPL        | CDPL     | LDPL     | CC                         |

Table 4 shows that all floors and building performance levels in Antalya, Isparta, Muğla, and Aydın provinces remain unchanged when the site-specific spectrum is used instead of the spectrum given in TBEC-2018 when only damage to beams is taken into account. In Burdur, while the performance level of the 1st floor, 2nd floor, and building was CPPL according to TBEC-2018, these performance levels became CDPL when the site-specific spectra were used. In Denizli, while 1st floor, 2nd floor, and building performance levels are CPPL according to TBEC-2018, these performance levels are CC if site-specific spectra are used. In İzmir, the use of a site-specific spectrum instead of the spectrum given in TBEC-2018 changed the performance level of the 2nd floor from CPPL to CC, the performance level of the 3rd floor from CDPL to CPPL, and the building performance level from CPPL to CC.

The performance levels obtained for the floors and the building according to the damage occurring only in the columns (considering the conditions given in Table 2 for columns only) are given in Table 5.

**Table 5.** Comparison of performance levels according to the damage to columns.

| Province | Used Spectrum Curve | Floor Performance Levels |          |             |          |          | Building Performance Level |
|----------|---------------------|--------------------------|----------|-------------|----------|----------|----------------------------|
|          |                     | 1. Floor                 | 2. Floor | 3. Floor    | 4. Floor | 5. Floor |                            |
| Antalya  | Site-specific       | CDPL                     | LDPL     | LDPL        | LDPL     | LDPL     | CDPL                       |
|          | TBEC-2018           | CDPL                     | LDPL     | LDPL        | LDPL     | LDPL     | CDPL                       |
| Isparta  | Site-specific       | CDPL                     | LDPL     | LDPL        | LDPL     | LDPL     | CDPL                       |
|          | TBEC-2018           | CDPL                     | LDPL     | LDPL        | LDPL     | LDPL     | CDPL                       |
| Burdur   | Site-specific       | <b>CDPL</b>              | LDPL     | LDPL        | LDPL     | LDPL     | <b>CDPL</b>                |
|          | TBEC-2018           | <b>CPPL</b>              | LDPL     | LDPL        | LDPL     | LDPL     | <b>CPPL</b>                |
| Denizli  | Site-specific       | CC                       | LDPL     | <b>CDPL</b> | CDPL     | LDPL     | CC                         |
|          | TBEC-2018           | CC                       | LDPL     | <b>LDPL</b> | CDPL     | LDPL     | CC                         |
| İzmir    | Site-specific       | CC                       | LDPL     | <b>CDPL</b> | CDPL     | LDPL     | CC                         |
|          | TBEC-2018           | CC                       | LDPL     | <b>LDPL</b> | CDPL     | LDPL     | CC                         |
| Muğla    | Site-specific       | CDPL                     | LDPL     | LDPL        | LDPL     | LDPL     | CDPL                       |
|          | TBEC-2018           | CDPL                     | LDPL     | LDPL        | LDPL     | LDPL     | CDPL                       |
| Aydın    | Site-specific       | CC                       | LDPL     | CDPL        | CDPL     | LDPL     | CC                         |
|          | TBEC-2018           | CC                       | LDPL     | CDPL        | CDPL     | CDPL     | CC                         |

As seen in Table 5, when only column damage is taken into consideration, it is seen that no floors or building performance levels are affected by the spectrum change in Antalya, Isparta, Muğla, and Aydın. In İzmir and Denizli, while the 3rd floor performance level was LDPL according to TBEC-2018, this performance level became CDPL when a site-specific spectrum was used. In Burdur, while the 1st floor and building performance levels are CPPL according to TBEC-2018, these performance levels became CDPL when a site-specific spectrum was used.

Considering both beam and column damage (considering all conditions in Table 2), the building performance levels obtained for provinces are given in Table 6.

**Table 6.** Comparison of building performance levels.

| Province | Used Spectrum Curve | Building Performance Level | Building Earthquake Safety |
|----------|---------------------|----------------------------|----------------------------|
| Antalya  | Site-specific       | CDPL                       | Safe                       |
|          | TBEC-2018           | CDPL                       | Safe                       |
| Isparta  | Site-specific       | CDPL                       | Safe                       |
|          | TBEC-2018           | CDPL                       | Safe                       |
| Burdur   | Site-specific       | <b>CDPL</b>                | <b>Safe</b>                |
|          | TBEC-2018           | <b>CPPL</b>                | <b>Unsafe</b>              |
| Denizli  | Site-specific       | CC                         | Unsafe                     |
|          | TBEC-2018           | CC                         | Unsafe                     |
| İzmir    | Site-specific       | CC                         | Unsafe                     |
|          | TBEC-2018           | CC                         | Unsafe                     |
| Muğla    | Site-specific       | CPPL                       | Unsafe                     |
|          | TBEC-2018           | CPPL                       | Unsafe                     |
| Aydın    | Site-specific       | CC                         | Unsafe                     |
|          | TBEC-2018           | CC                         | Unsafe                     |

According to TBEC-2018, residential buildings should meet the CDPL target performance for earthquake level with a return period of 475 years. The use of buildings that do not meet this performance level is not suitable for life safety. When Table 6 is analyzed, the building performance level of Burdur according to TBEC-2018 is CPPL, but this performance level is obtained as CDPL when a site-specific spectrum is used. Therefore, while the use of the building in Burdur according to TBEC-2018 is unsafe in terms of life safety, its use according to the site-specific spectrum is safe. Antalya, Isparta, Denizli, İzmir, Muğla, and Aydın are not affected by the change in the building performance level spectrum curve. According to both spectrum curves, the building is suitable for use in Antalya and Isparta in terms of life safety, while it is not suitable for use in Denizli, İzmir, Muğla, and Aydın in terms of life safety.

## 5. Conclusions and Discussion

This study examines the effect of using the site-specific spectrum instead of the elastic spectrum given in TBEC-2018 on building performance. In order to achieve this objective, spectrum curves were generated for earthquake levels with return periods of 2475, 475, and 72 years, corresponding to 2%, 10%, and 50% probability of exceedance in 50 years, respectively, for each urban center of provinces located in the southwest Anatolia region of Türkiye. The site-specific spectra were developed through the utilization of a detailed and comprehensive PSHA, which takes into account the seismotectonic characteristics of the region. Analytical models of a selected model RC building were created according to each province, and static pushover analyses of these building models were performed both according to the elastic spectra given in TBEC-2018 and the site-specific spectra for the province.

The results of the analyses show that the change in the spectrum changes the target displacement level of the buildings, and as a result, the cross-sectional damage zone of the structural elements under the earthquake effect is changed. So much so that using the site-specific instead of the elastic spectrum given in TBEC-2018 changed the damage zone of 43% of the beams and 26.4% of the columns in the İzmir model. The performance levels of some floors of the models and the building performance levels have changed due to the changes in the section damage zones. The biggest change in the building performance level due to the change in the spectrum curve was in the Burdur model. While the building performance level in Burdur was collapse prevention performance level according to TBEC-2018, this performance level became controlled damage performance level when the site-specific spectrum was used.

This study has revealed the importance of using the most realistic spectrum curves to obtain earthquake performance results of buildings that are as close as possible to the behavior of the buildings in a possible earthquake. The analyses in this study were performed considering a single building model whose purpose of use is residential. The change in the purpose of use of the building will require the use of different earthquake level elastic spectra (spectrum created using earthquakes with different return periods) in the performance analysis. It is planned to develop the study with building models with different structural characteristics and purposes of use in different site conditions. The use of spectrum curves obtained for different regions in the literature for the effects on building performance analysis will make these studies more meaningful. It is thought that conducting more studies on this subject will enable the comparison of studies similar to this study with each other.

**Author Contributions:** Conceptualization, M.A. and H.U.; methodology, M.A. and H.U.; software, M.A. and H.U.; validation, M.A. and H.U.; formal analysis, M.A. and H.U.; investigation, M.A. and H.U.; resources, M.A. and H.U.; data curation, M.A. and H.U.; writing—original draft preparation, M.A. and H.U.; writing—review and editing, M.A. and H.U.; visualization, M.A. and H.U.; supervision, M.A.; project administration, M.A. and H.U. All authors have read and agreed to the published version of the manuscript.

**Funding:** This research received no external funding.

**Data Availability Statement:** The data presented in this study are available on request from the corresponding author.

**Acknowledgments:** The authors would like to thank Andrzej Kijko for sharing the MATLAB codes used for the calculation of earthquake hazard parameters. The reviewers of the manuscript are thanked for their careful reading of the first version of the manuscript, their critical review, recommendations, and very helpful comments.

**Conflicts of Interest:** The authors declare no conflict of interest.

## References

- Alpyürür, M. Kayseri Kenti İçin Olasılıksal Sismik Tehlikenin Değerlendirilmesi. *Mehmet Akif Ersoy Üniv. Fen Bilim. Enstitüsü Derg.* **2022**, *14*, 1–15. [[CrossRef](#)]
- Yakut, A.; Sucuoğlu, H.; Akkar, S. Seismic Risk Prioritization of Residential Buildings in Istanbul. *Earthq. Eng. Struct. Dyn.* **2012**, *41*, 1533–1547. [[CrossRef](#)]
- Papazafeiropoulos, G.; Plevris, V. Kahramanmaraş-Gaziantep, Türkiye  $M_w$  7.8 Earthquake on 6 February 2023: Preliminary Report on Strong Ground Motion and Building Response Estimations. *Buildings* **2023**, *13*, 1194. [[CrossRef](#)]
- Arkan, E.; Işık, E.; Harirchian, E.; Topçubaşı, M.; Avcil, F. Architectural Characteristics and Determination Seismic Risk Priorities of Traditional Masonry Structures: A Case Study for Bitlis (Eastern Türkiye). *Buildings* **2023**, *13*, 1042. [[CrossRef](#)]
- Işık, E.; Işık, M.F.; Bülbül, M.A. Web Based Evaluation of Earthquake Damages for Reinforced Concrete Buildings. *Earthq. Struct.* **2017**, *13*, 423–432.
- Büyüksaraç, A.; Işık, E.; Harirchian, E.; Isik, E.; Harirchian, E. A Case Study for Determination of Seismic Risk Priorities in Van (Eastern Turkey). *Earthq. Struct.* **2021**, *20*, 445–455. [[CrossRef](#)]
- Özmen, B. Türkiye Deprem Bölgeleri Haritalarının Tarihsel Gelişimi. *Türkiye Jeol. Bülteni* **2012**, *55*, 43–55.
- Bilgin, H.; Hadzima-Nyarko, M.; Işık, E.; Ozmen, H.B.; Harirchian, E. A Comparative Study on the Seismic Provisions of Different Codes for RC Buildings. *Struct. Eng. Mech. An Int'l J.* **2022**, *83*, 195–206.
- TBEC, *Turkey Building Earthquake Code*; DEMP, Ministry of Interior, Disaster and Emergency Management Presidency: Ankara, Turkey, 2018.
- Akkar, S.; Azak, T.; Çan, T.; Çeken, U.; Demircioğlu Tümsa, M.B.; Duman, T.Y.; Erdik, M.; Ergintav, S.; Kadirioglu, F.T.; Kalafat, D.; et al. Evolution of Seismic Hazard Maps in Turkey. *Bull. Earthq. Eng.* **2018**, *16*, 3197–3228. [[CrossRef](#)]
- Akkar, S.; Kale, Ö.; Yakut, A.; Ceken, U. Ground-Motion Characterization for the Probabilistic Seismic Hazard Assessment in Turkey. *Bull. Earthq. Eng.* **2018**, *16*, 3439–3463. [[CrossRef](#)]
- Akkar, S.; Sandikkaya, M.A.; Bommer, J.J. Empirical Ground-Motion Models for Point- and Extended-Source Crustal Earthquake Scenarios in Europe and the Middle East. *Bull. Earthq. Eng.* **2014**, *12*, 359–387. [[CrossRef](#)]
- Yel, N.S.; Arslan, M.H.; Aksoylu, C.; Erkan, İ.H.; Arslan, H.D.; Işık, E. Investigation of the Earthquake Performance Adequacy of Low-Rise RC Structures Designed According to the Simplified Design Rules in TBEC-2019. *Buildings* **2022**, *12*, 1722. [[CrossRef](#)]
- Hu, Y.; Lam, N.; Khatiwada, P.; Menegon, S.J.; Looi, D.T.W. Site-Specific Response Spectra: Guidelines for Engineering Practice. *CivilEng* **2021**, *2*, 712–735. [[CrossRef](#)]
- Anbazhagan, P.; Bajaj, K.; Patel, S. Seismic Hazard Maps and Spectrum for Patna Considering Region-Specific Seismotectonic Parameters. *Nat. Hazards* **2015**, *78*, 1163–1195. [[CrossRef](#)]
- Li, B.; Cai, Z.; Xie, W.C.; Pandey, M. Probabilistic Seismic Hazard Analysis Considering Site-Specific Soil Effects. *Soil Dyn. Earthq. Eng.* **2018**, *105*, 103–113. [[CrossRef](#)]
- Ayele, A. Probabilistic Seismic Hazard Analysis (PSHA) for Ethiopia and the Neighboring Region. *J. Afr. Earth Sci.* **2017**, *134*, 257–264. [[CrossRef](#)]
- Silacheva, N.V.; Kulbayeva, U.K.; Kravchenko, N.A. Probabilistic Seismic Hazard Assessment of Kazakhstan and Almaty City in Peak Ground Accelerations. *Geod. Geodyn.* **2018**, *9*, 131–141. [[CrossRef](#)]
- Mäntyniemi, P.; Tsapanos, T.M.; Kijko, A. An Estimate of Probabilistic Seismic Hazard for Five Cities in Greece by Using the Parametric-Historic Procedure. *Eng. Geol.* **2004**, *72*, 217–231. [[CrossRef](#)]
- Zahran, H.M.; Sokolov, V.; Youssef, S.E.H.; Alraddadi, W.W. Preliminary Probabilistic Seismic Hazard Assessment for the Kingdom of Saudi Arabia Based on Combined Areal Source Model: Monte Carlo Approach and Sensitivity Analyses. *Soil Dyn. Earthq. Eng.* **2015**, *77*, 453–468. [[CrossRef](#)]
- Deniz, A.; Korkmaz, K.A.; Irfanoglu, A. Probabilistic Seismic Hazard Assessment for Izmir, Turkey. *Pure Appl. Geophys.* **2010**, *167*, 1475–1484. [[CrossRef](#)]
- Dipova, N.; Cangir, B. Probabilistic Seismic Hazard Assessment for the Two Layer Fault System of Antalya (SW Turkey) Area. *J. Seismol.* **2017**, *21*, 1067–1077. [[CrossRef](#)]
- İnce, G.Ç.; Yılmazoğlu, M.U. Probabilistic Seismic Hazard Assessment of Muğla, Turkey. *Nat. Hazards* **2021**, *107*, 1311–1340. [[CrossRef](#)]
- Alpyürür, M. Probabilistic Seismic Hazard Analysis of Burdur City. *Int. J. Eng. Appl. Sci.* **2023**, *14*, 91–99. [[CrossRef](#)]

25. Kırım, S.; Budakoğlu, E.; Horasan, G. Probabilistic Seismic Hazard Assessment for Isparta Province (Turkey) and Mapping Based on GIS. *Arab. J. Geosci.* **2021**, *14*, 2227. [[CrossRef](#)]
26. *TEC, Turkish Seismic Design Code*; Ministry of Public Works and Settlement, General Directorate of Disaster Affairs, Earthquake Research Department: Ankara, Turkey, 2007.
27. Ulutaş, H. DBYBHY (2007) ve TBDY (2018) Deprem Yönetmeliklerinin Kesit Hasar Sınırları Açısından Kıyaslanması. *Eur. J. Sci. Technol.* **2019**, *17*, 351–359. [[CrossRef](#)]
28. Işık, E.; Ulutaş, H.; Harirchian, E.; Avcil, F.; Aksoylu, C.; Arslan, M.H. Performance-Based Assessment of RC Building with Short Columns Due to the Different Design Principles. *Buildings* **2023**, *13*, 750. [[CrossRef](#)]
29. Işık, E.; Ulutaş, H.; Büyüksaraç, A. The Comparison of Sectional Damages in Reinforced-Concrete Structures and Seismic Parameters on Regional Basis; A Case Study from Western Türkiye (Aegean Region). *Earthq. Struct.* **2023**, *24*, 37–51. [[CrossRef](#)]
30. Prendergast, L.J.; Limongelli, M.P.; Ademovic, N.; Anžlin, A.; Gavin, K.; Zanini, M. Structural Health Monitoring for Performance Assessment of Bridges under Flooding and Seismic Actions. *Struct. Eng. Int.* **2018**, *28*, 296–307. [[CrossRef](#)]
31. Ademovic, N.; Hrasnica, M.; Oliveira, D.V. Pushover Analysis and Failure Pattern of a Typical Masonry Residential Building in Bosnia and Herzegovina. *Eng. Struct.* **2013**, *50*, 13–29. [[CrossRef](#)]
32. Avcil, F.; Işık, E.; İzol, R.; Büyüksaraç, A.; Arkan, E.; Arslan, M.H.; Aksoylu, C.; Eyisüren, O.; Harirchian, E. Effects of the February 6, 2023, Kahramanmaraş Earthquake on Structures in Kahramanmaraş City. *Nat. Hazards* **2023**, *120*, 2953–2991. [[CrossRef](#)]
33. Mertol, H.C.; Tunç, G.; Akış, T.; Kantekin, Y.; Aydın, İ.C. Investigation of RC Buildings after 6 February 2023, Kahramanmaraş, Türkiye Earthquakes. *Buildings* **2023**, *13*, 1789. [[CrossRef](#)]
34. Işık, E.; Avcil, F.; Büyüksaraç, A.; İzol, R.; Arslan, M.H.; Aksoylu, C.; Harirchian, E.; Eyisüren, O.; Arkan, E.; Güngür, M.Ş. Structural Damages in Masonry Buildings in Adıyaman during the Kahramanmaraş (Türkiye) Earthquakes (Mw 7.7 and Mw 7.6) on 06 February 2023. *Eng. Fail. Anal.* **2023**, *151*, 107405. [[CrossRef](#)]
35. Wang, T.; Chen, J.; Zhou, Y.; Wang, X.; Lin, X.; Wang, X.; Shang, Q. Preliminary Investigation of Building Damage in Hatay under February 6, 2023 Turkey Earthquakes. *Earthq. Eng. Eng. Vib.* **2023**, *22*, 853–866. [[CrossRef](#)]
36. Kutanis, M.; Ulutaş, H.; Işık, E. PSHA of Van Province for Performance Assessment Using Spectrally Matched Strong Ground Motion Records. *J. Earth Syst. Sci.* **2018**, *127*, 99. [[CrossRef](#)]
37. Işık, E.; Kutanis, M. Determination of Local Site-Specific Spectra Using Probabilistic Seismic Hazard Analysis for Bitlis Province, Turkey. *Earth Sci. Res. J.* **2015**, *19*, 129–134. [[CrossRef](#)]
38. Bozkurt, E. Neotectonics of Turkey—a Synthesis. *Geodin. Acta* **2001**, *14*, 3–30. [[CrossRef](#)]
39. Barka, A.A.; Kadinsky-Cade, K. Strike-slip Fault Geometry in Turkey and Its Influence on Earthquake Activity. *Tectonics* **1988**, *7*, 663–684. [[CrossRef](#)]
40. Şengör, A.M.C.; Görür, N.; Şaroğlu, F. Strike-Slip Faulting and Related Basin Formation in Zones of Tectonic Escape: Turkey as a Case Study. In *Strike-Slip Deformation, Basin Formation, and Sedimentation*; Society of Economic Paleontologists and Mineralogists: Tulsa, OK, USA, 1985; Volume 37.
41. Seyitoğlu, G.; Scott, B.C.; Rundle, C.C. Timing of Cenozoic Extensional Tectonics in West Turkey. *J. Geol. Soc.* **1992**, *149*, 533–538. [[CrossRef](#)]
42. Seyitoğlu, G.; Scott, B.C. The Cause of N-S Extensional Tectonics in Western Turkey: Tectonic Escape vs Back-Arc Spreading vs Orogenic Collapse. *J. Geodyn.* **1996**, *22*, 145–153. [[CrossRef](#)]
43. Gürer, Ö.F.; Sarica-Filoreau, N.; Özbüran, M.; Sangu, E.; Doğan, B. Progressive Development of the Büyük Menderes Graben Based on New Data, Western Turkey. *Geol. Mag.* **2009**, *146*, 652–673. [[CrossRef](#)]
44. Kürçer, A.; Özdemir, E.; Olgun, Ş.; Özalp, S.; Çan, T.; Elmacı, H. Active Tectonic and Paleoseismological Characteristics of the Dinar Fault, SW Anatolia, Turkey. *Mediterr. Geosci. Rev.* **2021**, *3*, 219–251. [[CrossRef](#)]
45. Paton, S. Active Normal Faulting, Drainage Patterns and Sedimentation in Southwestern Turkey. *J. Geol. Soc.* **1992**, *149*, 1031–1044. [[CrossRef](#)]
46. Kırkan, E.; Akyüz, H.S.; Basmenji, M.; Dikbaş, A.; Zabcı, C.; Yazıcı, M.; Erturaç, M.K. Earthquake History of the Milas Fault: An Active Dextral Fault in an Extensional Province (SW Anatolia, Türkiye). *Nat. Hazards* **2023**, *116*, 1639–1662. [[CrossRef](#)]
47. Barka, A.; Reilinger, R. Active Tectonics of the Eastern Mediterranean Region: Deduced from GPS, Neotectonic and Seismicity Data. *Ann. Geophys.* **1997**, *40*, 587–610. [[CrossRef](#)]
48. Reilinger, R.; McClusky, S.; Vernant, P.; Lawrence, S.; Ergintav, S.; Cakmak, R.; Ozener, H.; Kadirov, F.; Guliev, I.; Stepanyan, R.; et al. GPS Constraints on Continental Deformation in the Africa-Arabia-Eurasia Continental Collision Zone and Implications for the Dynamics of Plate Interactions. *J. Geophys. Res. Solid Earth* **2006**, *111*. [[CrossRef](#)]
49. Basmenji, M.; Akyüz, H.S.; Kırkan, E.; Aksoy, M.E.; Uçarkuş, G.; Yakupoğlu, N. Earthquake History of the Yatağan Fault (Muğla, Sw Turkey): Implications for Regional Seismic Hazard Assessment and Paleoseismology in Extensional Provinces. *Turkish J. Earth Sci.* **2021**, *30*, 161–181. [[CrossRef](#)]
50. Şengör, A.M.C. Cross-Faults and Differential Stretching of Hanging Walls in Regions of Low-Angle Normal Faulting: Examples from Western Turkey. *Geol. Soc. Spec. Publ.* **1987**, *28*, 575–589. [[CrossRef](#)]
51. Yılmaz, Y.; Genç, Ş.C.; Gürer, F.; Bozcu, M.; Yılmaz, K.; Karacik, Z.; Altunkaynak, Ş.; Elmas, A. When Did the Western Anatolian Grabens Begin to Develop? *Geol. Soc. Spec. Publ.* **2000**, *173*, 353–384. [[CrossRef](#)]
52. Emre, Ö.; Duman, T.Y.; Özalp, S.; Şaroğlu, F.; Olgun, Ş.; Elmacı, H.; Çan, T. Active Fault Database of Turkey. *Bull. Earthq. Eng.* **2018**, *16*, 3229–3275. [[CrossRef](#)]

53. Meng, J.; Sinoplu, O.; Zhou, Z.; Tokay, B.; Kusky, T.; Bozkurt, E.; Wang, L. Greece and Turkey Shaken by African Tectonic Retreat. *Sci. Rep.* **2021**, *11*, 6486. [[CrossRef](#)]
54. Cohen, H.A.; Dart, C.J.; Akyuz, H.S.; Barka, A. Syn-Rift Sedimentation and Structural Development of the Gediz and Buyuk Menderes Graben, Western Turkey. *J. Geol. Soc.* **1995**, *152*, 629–638. [[CrossRef](#)]
55. Hetzel, R.; Ring, U.; Akal, C.; Troesch, M. Miocene NNE-Directed Extensional Unroofing in the Menderes Massif, Southwestern Turkey. *J. Geol. Soc.* **1995**, *152*, 639–654. [[CrossRef](#)]
56. Hetzel, R.; Romer, R.L.; Candan, O.; Passchier, C.W. Geology of the Bozdag Area, Central Menderes Massif, SW Turkey: Pan-African Basement and Alpine Deformation. *Geol. Rundsch.* **1998**, *87*, 394–406. [[CrossRef](#)]
57. Van Hinsbergen, D.J.J.; Schmid, S.M. Map View Restoration of Aegean-West Anatolian Accretion and Extension since the Eocene. *Tectonics* **2012**, *31*, TC5005. [[CrossRef](#)]
58. Türe, O.; Çobanoğlu, İ.; Gül, M.; Karacan, E. Seismic Record Approach for the Evaluation of Natural Hazards: A Key Study from SW Anatolia/Turkey. *Environ. Earth Sci.* **2021**, *80*, 500. [[CrossRef](#)]
59. Stucchi, M.; Rovida, A.; Gomez Capera, A.A.; Alexandre, P.; Camelbeeck, T.; Demircioglu, M.B.; Gasperini, P.; Kouskouna, V.; Musson, R.M.W.; Radulian, M.; et al. The SHARE European Earthquake Catalogue (SHEEC) 1000-1899. *J. Seismol.* **2013**, *17*, 523–544. [[CrossRef](#)]
60. Bommer, J.J.; Abrahamson, N.A. Why Do Modern Probabilistic Seismic-Hazard Analyses Often Lead to Increased Hazard Estimates? *Bull. Seismol. Soc. Am.* **2006**, *96*, 1967–1977. [[CrossRef](#)]
61. McGuire, R.K. Probabilistic Seismic Hazard Analysis: Early History. *Earthq. Eng. Struct. Dyn.* **2008**, *37*, 329–338. [[CrossRef](#)]
62. Cornell, C.A. Engineering Seismic Risk Analysis. *Bull. Seismol. Soc. Am.* **1968**, *58*, 1583–1606. [[CrossRef](#)]
63. Kijko, A.; Smit, A. Extension of the Aki-Utsu b-Value Estimator for Incomplete Catalogs. *Bull. Seismol. Soc. Am.* **2012**, *102*, 1283–1287. [[CrossRef](#)]
64. Anbazhagan, P.; Bajaj, K.; Moustafa, S.S.R.; Al-Arifi, N.S.N. Maximum Magnitude Estimation Considering the Regional Rupture Character. *J. Seismol.* **2015**, *19*, 695–719. [[CrossRef](#)]
65. Kijko, A.; Sellevoll, M.A. Estimation of Earthquake Hazard Parameters from Incomplete Data Files. Part I. Utilization of Extreme and Complete Catalogs with Different Threshold Magnitudes. *Bull. Seismol. Soc. Am.* **1989**, *79*, 645–654. [[CrossRef](#)]
66. Weichert, D.H. Estimation of the Earthquake Recurrence Parameters for Unequal Observation Periods for Different Magnitudes. *Bull. Seismol. Soc. Am.* **1980**, *70*, 1337–1346. [[CrossRef](#)]
67. Tinti, S.; Mulargia, F. Effects of Magnitude Uncertainties on Estimating the Parameters in the Gutenberg-Richter Frequency-Magnitude Law. *Bull. Seismol. Soc. Am.* **1985**, *75*, 1681–1697. [[CrossRef](#)]
68. Kijko, A. *Ha3 Matlab Code, Released 3.01*; Seismic Hazard Assessment for Selected Area; University of Pretoria: Pretoria, South Africa, 2016.
69. İlki, A.; Celep, Z. Betonarme Yapıların Deprem Güvenliği. In Proceedings of the 1st Turkish Earthquake Engineering and Seismology Conference, Ankara, Turkey, 11–14 October 2011.
70. SAP2000. *Integrated Software for Structural Analysis & Design*; Computers & Structures, Inc.: Berkeley, CA, USA, 2011.

**Disclaimer/Publisher’s Note:** The statements, opinions and data contained in all publications are solely those of the individual author(s) and contributor(s) and not of MDPI and/or the editor(s). MDPI and/or the editor(s) disclaim responsibility for any injury to people or property resulting from any ideas, methods, instructions or products referred to in the content.